ELECTRICAL RESISTIVITY STUDIES OF FORTYMILE WASH, NYE COUNTY, NEVADA

Prepared for

U.S. Nuclear Regulatory Commission
Contract NRC–02–02–012

Prepared by

David A. Farrell
Center for Nuclear Waste Regulatory Analyses
San Antonio, Texas

Stewart K. Sandberg
Geophysical Solutions
Albuquerque, New Mexico

December 2003

ABSTRACT

This report provides a summary of recent direct current electrical resistivity, induced polarization, and time-domain electromagnetic studies performed in southern Fortymile Wash and neighboring northern Amargosa Valley, Nevada, in 1998 and 1999 by the Center for Nuclear Waste Regulatory Analyses staff. The 1998 study was designed to investigate the applicability of the time-domain electromagnetic method to map the water table and hydrostratigraphic features in the region. The followup study in 1999 extended the 1998 investigations through the inclusion of induced polarization and direct current electrical resistivity methods. Data from the 1999 survey were interpreted using a simultaneous inversion strategy, where applicable, in an effort to minimize geophysical modeling nonuniqueness. The report shows that when good constraints are available through either multiple geophysical data sets or good geologic data, the simultaneous inversion strategy provides a reasonable approach for imaging the broad structure of the water table. Unfortunately, for the level of accuracy required for groundwater flow models in the Yucca Mountain region and given the shallow groundwater gradients, the errors in the inferred elevations of the water table were generally too large {5–20 m [16–65 ft]} to support detailed modeling of groundwater flow in the region. As shown in the report, however, the approach may be suitable for constraining the hydrostratigraphy south of Fortymile Wash.

CONTENTS

FIGURES

TABLES

ACKNOWLEDGMENTS

This report was prepared to document work performed by the Center for Nuclear Waste Regulatory Analyses (CNWRA) for the U.S. Nuclear Regulatory Commission (NRC) under Contract No. NRC–02–02–012. The activities reported here were performed on behalf of the NRC Office of Nuclear Material Safety and Safeguards, Division of Waste Management. The views expressed in the report are those of the authors and do not necessarily reflect the views or regulatory position of NRC.

The authors gratefully acknowledge R. Green for technical review, the programmatic review of J. Russell, and the editorial reviews of C. Cudd and B. Long. Appreciation is due to P. Houston for assistance in preparing this report. The authors are appreciative of the informal reviews and suggestions provided by D. Sims, A. Morris, and B. Hill. The authors are also appreciative of P. LaFemina and C. Connor for their help in execution of the field work.

QUALITY OF DATA, ANALYSES, AND CODE DEVELOPMENT

QUALITY OF DATA: Data collected during the 1998 and 1999 geophysical surveys that form the basis of this report were processed by Dr. Stewart Sandberg, Geophysical Solutions, Inc., according to a consulting agreement with CNWRA. Processing of these data is summarized in Sandberg (2000, 1998a), prepared by Geophysical Solutions, Inc. for CNWRA. Data associated with the 1999 geophysical field survey are contained in CNWRA Scientific Notebook 317E (Farrell, 2000). Additional support data are contained on the computer Medusa (Room 212A, Bldg. 189, Southwest Research Institute®) in directory d:\emproj\1999-survey-data. Field and processed data for the 1998 field survey [described in this report and Sandberg (1998a)] are contained in d:\emproj\1998-survey-data. Summaries of the electrical resistivity models developed in Sandberg (2000, 1998a) based on data collected during the 1998 and 1999 surveys are summarized in the attached appendix. Nye County Early Warning Drilling Program well data used in the report were obtained from http://www.nyecounty.com/ewdpmain.htm. The source of the Nye County Early Warning Drilling Program data should be consulted to determine the level of quality of the data. Data used to support this project also are stored at CNWRA on a compact disk associated with this report in the CNWRA quality assurance system.

ANALYSES AND CODES: The suite of codes (ZONGE, READZONG, T47INPUT, READ, SLUMBER, RAMPRES3, AND EINVRT6) described in Sandberg (1998b) was used to process the field geophysical data collected. This suite of codes is controlled following the procedures described in the CNWRA Technical Operating Procedure 18, which implements the quality assurance guidance contained in the CNWRA quality assurance manual. One-time use only scripts used to reorganize the Nye County Early Warning Drilling Program well data are stored at CNWRA on the computer Medusa (Room 212A) in directories d:\emproj\1999-survey-data-ncewdp-10S, d:\emproj\1999-survey-data-ncewdp-2DB, d:\emproj\1999-survey-data-ncewdp-23p, and d:\emproj\1999-survey-data-ncewdp-4p. These data are also stored on a compact disk associated with this report in the CNWRA quality assurance system.

References

Farrell, D.A. "Scientific Notebook #317E: Subsurface Electrical Conductivity Mapping of Fortymile Wash and the Amargosa Desert (03/18/1999–02/28/2000)." San Antonio, Texas: CNWRA. 2000.

Sandberg, S.K. "Final Report: Geophysical Survey at Fortymile Wash, Yucca Mountain, Nevada: Geophysical Solutions." San Antonio, Texas: CNWRA. 2000.

———. "Draft Report on Modeling TEM Data from Nevada." Albuquerque, New Mexico: Geophysical Solutions. 1998a.

———. "Inverse Modeling Software for Resistivity, Induced Polarization (IP), and Transient Electromagnetic (TEM, TDEM) Soundings: Manual for Computer Programs, ZONGE, READZONG, T47INPUT, READ, SLUMBER, RAMPRES3, EINVRT6 (MS-DOS Version 6.0)." Albuquerque, New Mexico: Geophysical Solutions. 1998b.

1 INTRODUCTION

Yucca Mountain, Nye County, Nevada, is being characterized by the U.S. Department of Energy (DOE) as a potential location for an underground high-level waste repository. The saturated zone extending from Yucca Mountain to southern Fortymile Wash and northern Amargosa Valley is considered an important component of the natural barrier system to radionuclide migration.

Current groundwater flow and mass transport models proposed for the saturated zone at Yucca Mountain (Winterle, 2003; Winterle, et al., 2002; CRWMS M&O, 2000) indicate that, should radionuclides enter the saturated zone below the proposed repository location, transport initially would be toward the southeast prior to a more southerly route through southern Fortymile Wash and northern Amargosa Valley (Figure 1-1) and subsequent to extraction at a pumping well at the location of the reasonably maximally exposed individual, approximately 18 km [11.2 mi] away (see 10 CFR 63.1, 63.302, 63.311, and 63.312). In southern Fortymile Wash, currently it is postulated that groundwater flows from a fractured tuff aquifer system to a valley-fill aquifer system. The transition from fractured tuff to valley-fill is significant for repository performance because of contrasting hydrologic and geochemical properties of the two media. It is currently estimated that groundwater velocities through the valley-fill system will be significantly lower than those in the fractured tuff system (Winterle, et al., 2002). Hence, depending on the ratio of the radionuclide travel path in the fractured tuff to that in the valley-fill, significant residence times within the valley-fill are possible. Longer radionuclide residence times in the valley-fill, coupled with the greater surface for radionuclide sorption, could delay and reduce radionuclide concentrations at the location of the reasonably maximally exposed individual (10 CFR 63.1, 63.302, 63.311, and 63.312).

Although the potential importance of southern Fortymile Wash and northern Amargosa Valley to repository safety performance is recognized, the geologic and hydrogeologic structure of the region is not well characterized. Prior to the start of the Nye County Early Warning Drilling Program in 1999, insufficient data were available to characterize the structural geology and hydrogeology of the Fortymile Wash region. Because of the limited hydrogeologic and geologic data available for the wash, there is considerable uncertainty in the (i) location of the tuff and valley-fill interface, (ii) hydraulic gradients to the south of the repository, and (iii) general geologic and, consequently, hydrogeologic structure of the region. Reduction of these uncertainties can help to improve repository safety assessments.

Noninvasive geophysical surveys have been conducted for the past 30 years to characterize the geology of southern Fortymile Wash and neighboring northern Amargosa Valley. Only a few of these studies addressed the hydrogeologic features of southern Fortymile Wash and northern Amargosa Valley. Beginning in 1998, and prior to the Nye County Early Warning Drilling Program, the U.S. Nuclear Regulatory Commission (NRC) funded two electrical resistivity geophysical surveys to verify and better constrain the hydrogeologic structure of the southern Fortymile Wash and northern Amargosa Valley to independently evaluate repository performance. This report summarizes those two surveys and the results. Where appropriate, the report also discusses research findings from other groups. Results from the Nye County Early Warning Drilling Program are used to verify models inferred from the geophysical data.

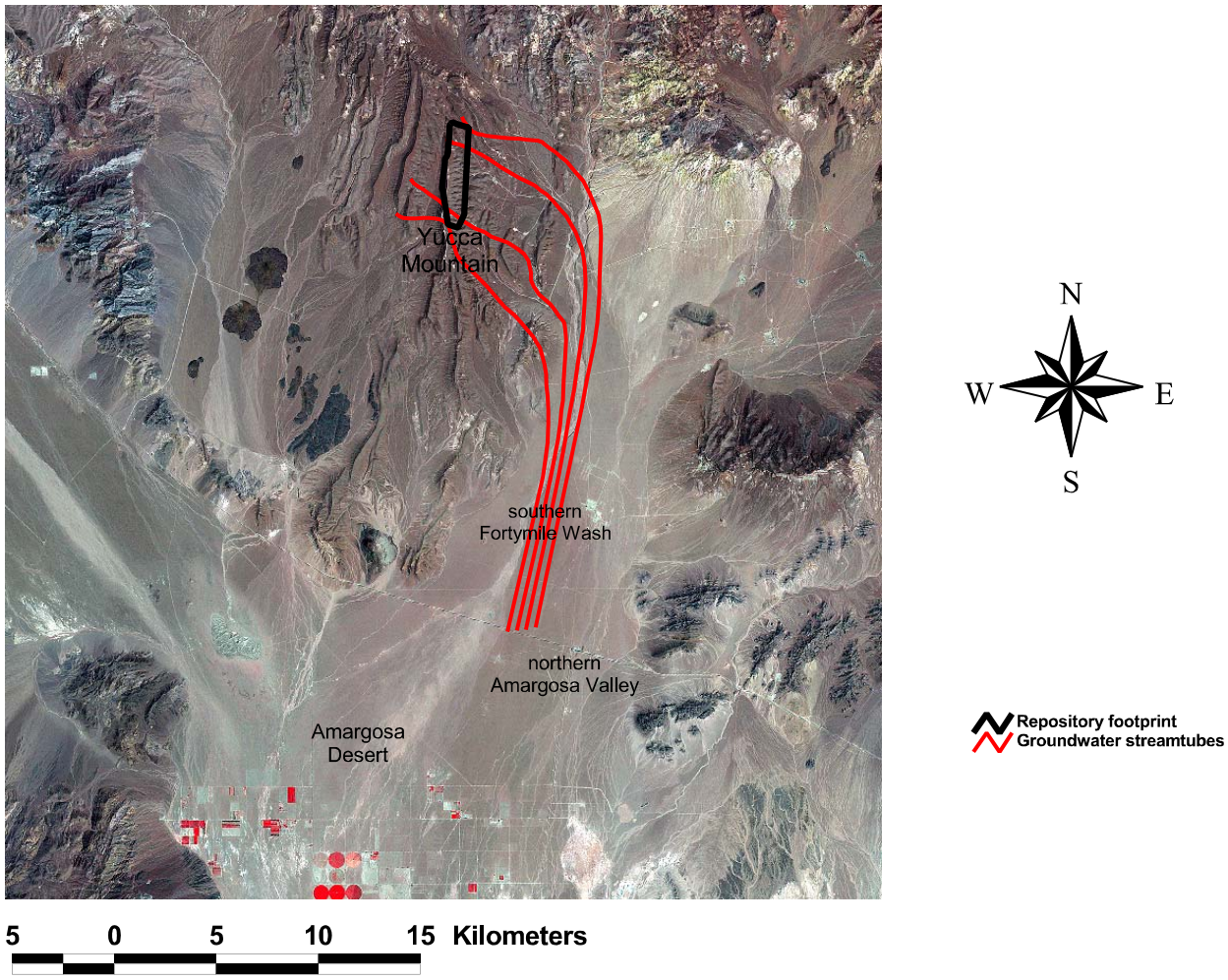

Figure 1-1. Southern Fortymile Wash and Northern Amargosa Valley Showing the Locations of Nye County Early Warning Drilling Program Wells and Groundwater Streamtubes Used in the TPA Version 4.0 Code (Mohanty, et al., 2000). NOTE: Scale information provided in kilometers; for conversion use 1 km = 0.621 m. Background image based on LandSat7 satellite image of the Yucca Mountain region.

Chapter 2 of this report summarizes previous electrical resistivity studies in southern Fortymile Wash and neighboring northern Amargosa Valley. Chapter 3 summarizes electrical and electromagnetic studies performed across southern Fortymile Wash and northern Amargosa Valley by the Center for Nuclear Waste Regulatory Analyses (CNWRA) staff that were designed to infer the electrical resistivity and hydrogeologic structure of the region. Chapter 4 summarizes the results of this work and suggests possible paths forward.

It is important to note that, in addition to the electrical resistivity surveys described in this report, the CNWRA staff also performed a suite of gravity and magnetic surveys across southern Fortymile Wash and northern Amargosa Valley designed to map larger-scale and deeper targets that control the structure of the region. These surveys are not discussed in this report but will be discussed in a future report. To the extent possible, the future report will compare

results from this report with models based on the gravity and magnetic surveys across the region in an effort to develop a consistent hydrogeologic and geologic model for the region. This approach will, therefore, reduce geologic model nonuniqueness that commonly arises in the interpretation of geophysical data when few constraints are available.

Although the surveys were performed prior to development of the Unsaturated and Saturated Flow Under Isothermal Conditions Key Technical Issue agreement USFIC .5.04 and Radionuclide Transport Key Technical Issue agreements RT.2.08 and RT.3.03 (Reamer, 2000a,b) between DOE and NRC, results from this report and the planned future report on the CNWRA gravity and magnetic studies in the region may provide useful information to assist staff in addressing these agreements.

2 PREVIOUS ELECTRICAL AND ELECTROMAGNETIC RESISTIVITY STUDIES IN FORTYMILE WASH AND NORTHERN AMARGOSA VALLEY

Prior to the CNWRA electrical resistivity studies in southern Fortymile Wash and northern Amargosa Valley, several geophysical studies were performed in the region by various research groups to map the electrical resistivity structure of the region. The objectives of these studies ranged from structural mapping to hydrological characterization. This chapter summaries these studies as part of the background for this work. Summaries of some of these studies also are provided in Farrell, et al. (1999). These studies included telluric surveys and Schlumberger direct current (D.C.) electrical resistivity depth-soundings.

2.1 Telluric Studies

Telluric methods map electrical potential differences in the subsurface that result from subsurface current flows induced by varying ionospheric current flows. Higher frequency current fluctuations caused by electrical storms may be superimposed on the natural long-wavelength telluric currents.

Telluric studies conducted in the Yucca Mountain region and, more specifically, southern Fortymile Wash and northern Amargosa Valley by Hoover, et al. (1982) consisted of four east-west trending lines (Figure 2-1): two lines that extend from the area of Yucca Mountain, across Fortymile Wash and into Jackass Flats (transects Line 1 and Line 2), and two additional lines located in northern Amargosa Valley (transects L-N and L-S).

Line 1 of the survey (Figure 2-1; see also Hoover, et al., 1982) was located 0.6 km [0.4 mi] north of Well J–13 and approximately 3 km [1.8 mi] south of Line 2 (Figure 2-1). Within southern Fortymile Wash, data collected along these two transects identified four north-south trending lineaments [Figure 2-1 (two on either side of the wash)] of low telluric voltages indicative of low earth electrical resistivity. Hoover, et al. (1982) described these lineaments as possible fault zones and asserted the lower electrical resistivity along these features may result from increased porosity associated with fracturing. If this is indeed the case, the enhanced porosities along these faults may explain enhanced transmissivities observed in Fortymile Wash. Hoover, et al. (1982) further suggested that if the assertion that Fortymile Wash is fault controlled [Lipman and Mackay (1965)] and Well J–13 is assumed to lie within a graben, the inner lineations interpreted in the telluric profiles could define the Fortymile Wash graben. Farrell, et al. (1999) noted the westernmost of the four faults correlates reasonably well with the general location of Paintbrush fault.

The telluric transect L-N (Figure 2-1), north of the town of Amargosa Valley (Lathrop Wells), identified several contrasting responses (Hoover, et al., 1982). West of point 6E on this line, low telluric voltages occur; whereas, immediately east of this location, higher voltages occur. This gradient was interpreted by Hoover, et al. (1982) to represent carbonate rocks to the east juxtaposed with alluvium (valley-fill), and possible volcanics, to the west. This contact appears to be coincident with the known location of the Gravity fault (Farrell, et al., 1999). Possible faulting between 1W and 3E along line L-N also may be inferred from the data (Farrell, et al., 1999).

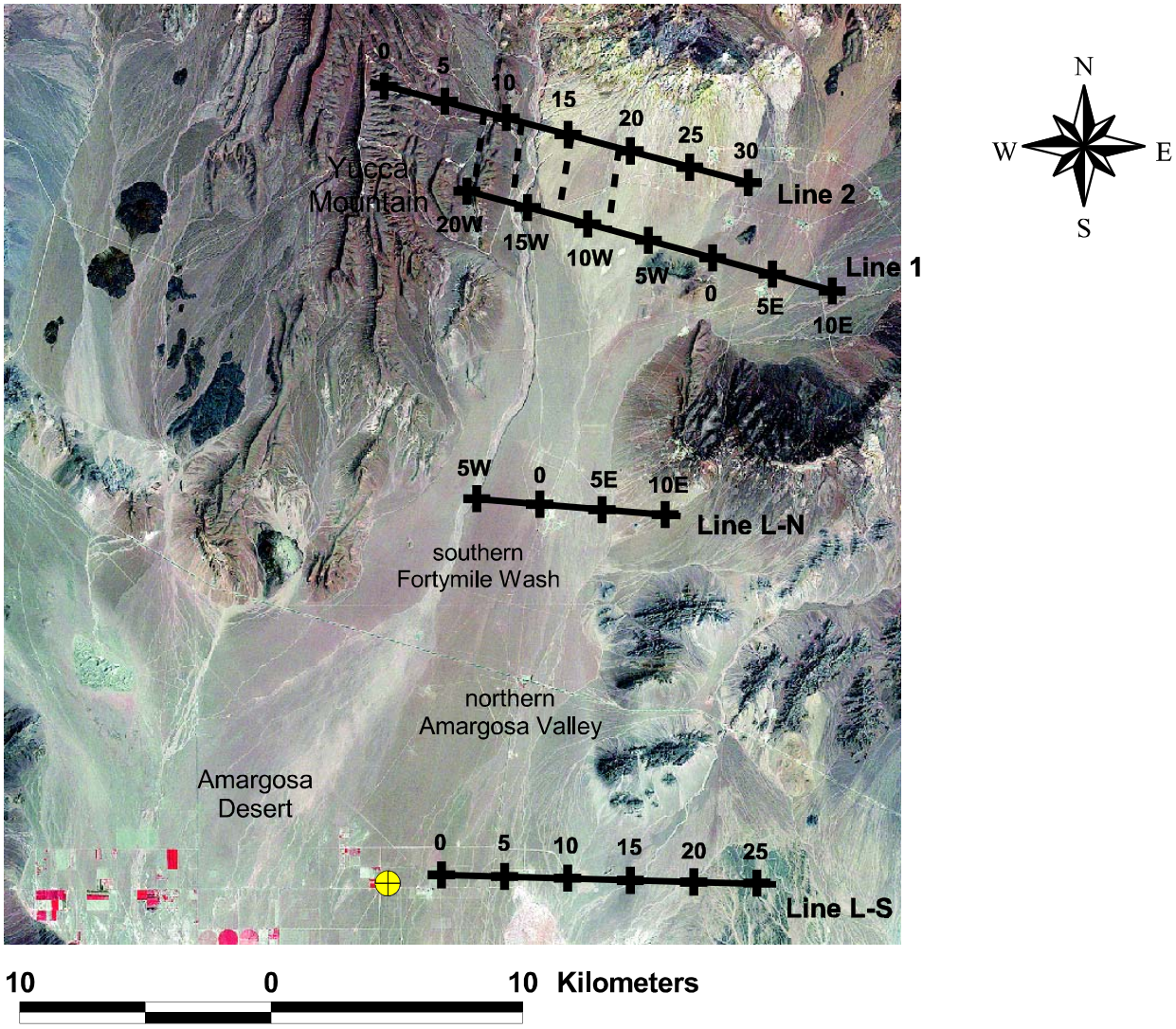

Figure 2-1. Approximate Locations of the Telluric Transects Described in Hoover, et al. (1982).
NOTE: Scale information provided in kilometers; for conversion use 1 km = 0.621 m. Background image based on LandSat7 satellite image of the Yucca Mountain region.

Telluric transect L-S (Figure 2-1), located south of the town of Amargosa Valley, is almost coincident with the joint seismic and gravity line AV–1 (Brocher, et al., 1990). Along Line L-S, the voltage gradient observed near point 12 appears to correlate to the general location of the Gravity fault.

2.2 Schlumberger D.C. Electrical Resistivity Depth-Sounding Studies

From 1978 through 1980, the U.S. Geological Survey performed 136 Schlumberger D.C. electrical resistivity depth-soundings across Amargosa Desert, Ash Meadows, southern Fortymile Wash, and northern Amargosa Valley. These soundings were performed as part of the initial site characterization for the proposed repository at Yucca Mountain. The objectives of the soundings were to define the basement structure and basin characteristics that may influence hydrological systems in the region (Greenhaus and Zablocki, 1982). Because of the anticipated deep basement, maximum current electrode spacings at each sounding location ranged from 1,219 to 2,438 m [4,000 to 8,000 ft]. Additional data collection strategies included (i) using crossed pairs of soundings at several locations to identify anisotropy and (ii) reoccupying some sounding locations with an extended array to support deeper penetration.

The depth to electrical basement modeled in this work may differ from the true geologic basement. As noted by Greenhaus and Zablocki (1982), depths to the electrical and geological basements will generally be consistent if there is no alteration of the bedrock contact surface. If the uppermost part of the geological basement has been extensively fractured, however, such that the secondary porosity produced may become either filled with clay-rich sediments or water, the reduced electrical resistivity in this zone may preclude it being modeled as part of the electrical basement. That is, the top of the electrical basement will be interpreted to be below this layer of high fracturing.

Greenhaus and Zablocki (1982) made the following observations based on their analyses of the electrical resistivity soundings. They observed that a significant electrical resistivity gradient existed east of Fortymile Wash and south of the town of Amargosa Valley (Lathrop Wells). They concluded this feature represented a north-south trending normal fault, with an 800-m [2,625-ft] down-throw to the west. The location of this fault is consistent with the location of the Gravity fault.

The second observation of Greenhaus and Zablocki (1982) relates to the sources of the observed electrical resistivity anomalies. On the basis of existing borehole logs, the authors assumed the valley-fill was composed of heterogeneous distributions of clay, sand, gravel, and boulders. Near-surface high resistivities on the order of 10–100 ohm-m were assumed to represent dry surficial sands and gravels. North of U.S. Highway 95, the thickness of the high electrical resistivity zone was observed on the order of 100 m [328 ft]. This thickness is in reasonable agreement with recent data obtained from the Nye County Early Warning Drilling Project wells for southern Fortymile Wash. Beneath this zone, electrical resistivities on the order of 10–100 ohm-m were assumed to represent sands and clay-rich sediments, and electrical resistivities less than 10 ohm-m were assumed to represent saturated clays or saline groundwater.

The third observation of Greenhaus and Zablocki (1982) concerns the thick low electrical resistivity zone located on the down-thrown side of the Gravity fault. Electrical resistivities beneath the near-surface high electrical resistivity zone represent some of the lowest electrical resistivities in the surveyed area (estimated at approximately 10 ohm-m). Greenhaus and Zablocki (1982) concluded this zone may represent several hundred feet of either clay-rich sediments or saline groundwater above the electrical basement. The presence of a thick

sequence of clay-rich sediment in this general area appears to have been confirmed by geologic logs from Nye County Early Warning Drilling Program Wells 5S and 5SB.

The findings of Greenhaus and Zablocki (1982) have been used in subsequent synthesis reports that attempt to describe the depth to basement in the Amargosa Desert and Fortymile Wash regions (e.g., Oatfield and Czarnecki, 1989). The work of Oatfield and Czarnecki (1989) is interesting because it attempts to infer hydrologic relations from geophysical and grain-size analysis data. The following summarizes the findings of Oatfield and Czarnecki (1989) with respect to electrical resistivity.

In their analyses, Oatfield and Czarnecki (1989) assumed the electrical resistivity of the valley-fill is controlled by three factors: (i) salinity of the groundwater, (ii) degree of saturation, and (iii) electrical conductivity of the mineral grains. Also, it was assumed the electrical resistivity of the electrical basement is significantly larger than that of the overlying sediment. This assumption is consistent with the findings of Greenhaus and Zablocki (1982).

As part of their analyses, Oatfield and Czarnecki (1989) also computed an average transverse electrical resistivity, R, for the valley-fill at each of the vertical electrical resistivity profiles produced by Greenhaus and Zablocki (1982), using the following formulation

$$R = \frac{\sum_{i=1}^{n} r_i t_i}{\sum_{i=1}^{n} t_i} \qquad (2\text{-}1)$$

where

r_i and t_i — electrical resistivity and thickness of layer i
n — number of layers

It is important to note a representative value of R for the alluvium (valley-fill) is only valid provided the profile extends across the entire thickness of the alluvium (valley-fill). If this is not the case, the thickness of layer n cannot be defined. Hence, this approach cannot be applied to the profiles for alluvium computed in the CNWRA analyses described later in this report.

The estimate of R for southern Fortymile Wash, northern Amargosa Valley, and central Amargosa Desert represented some of the lowest values calculated. This result was described by Oatfield and Czarnecki (1989) as unexpected because it was counter to the trend in grain-size measurements and sodium concentrations observed. As an additional analysis, Oatfield and Czarnecki (1989) computed R for the upper 75 m [246 ft] of valley-fill. The depth of 75 m [246 ft] was chosen to be consistent with the depth of water wells used for grain-size analyses (Oatfield and Czarnecki, 1989). Contours of the recomputed values of R using this approach were described as more consistent with the spatial distribution of sodium. Results from the recomputed values of R were interpreted as indicating fresher waters and, hence, higher average transverse electrical resistivities beneath southern Fortymile Wash, northern Amargosa Valley, and the central Amargosa Desert.

In reality, the average transverse electrical resistivity computed by Oatfield and Czarnecki (1989) is difficult to interpret in the manner proposed. As mentioned earlier, the parameter is influenced to varying degrees by saturation, mineral conductivity, and salinity. The relative importance of each of these factors is masked in the value of R. As a result, it is not surprising that some of the trends and correlations noted by Oatfield and Czarnecki (1989) are not readily apparent. For example, Oatfield and Czarnecki (1989) expressed surprise that some of the lowest R values were observed in southern Fortymile Wash, northern Amargosa Valley, and central Amargosa Desert. In their opinion, this observation is contrary to the observed grain-size distributions and sodium concentrations. This is not surprising, however, given the shallowest groundwater depths occur in these regions, and small values of t_i significantly increase R. An alternate approach that could yield improved correlations and minimize the impact of the unsaturated zone on the calculated value is to compute R for the region below the water table.

3 CNWRA ELECTRICAL AND ELECTROMAGNETIC RESISTIVITY STUDIES IN FORTYMILE WASH AND NORTHERN AMARGOSA VALLEY

The geology and hydrogeology of Southern Fortymile Wash and northern Amargosa Valley are not well characterized and understood. In recent years, data from the Nye County Early Warning Drilling Program have increased the level of characterization in this region. Information taken from the wells being installed under this program, even when combined with other existing wells and available data, does not eliminate significant uncertainty with regard to flow paths in the valley-fill.

Prior to initiation of the Nye County Early Warning Drilling Program, large spatial gaps existed in the hydrogeologic and geologic data sets for southern Fortymile Wash and northern Amargosa Valley and the Amargosa Desert. In some areas viewed as important to evaluating the safety performance of the proposed repository, separations greater than 10 km [6.2 mi] existed between adjacent water level measurements. To reduce the uncertainty in the hydrogeology and geology of the region and to verify existing and future DOE groundwater flow and radionuclide transport for this region, a suite of noninvasive field geophysical surveys was planned and executed during 1998–1999 by the CNWRA staff. These surveys coincided with the initiation and early development of the Nye County Early Warning Drilling Program. It is important to note that although the surveys were performed prior to Unsaturated and Saturated Flow Under Isothermal Conditions agreement USFIC.5.04 and Radionuclide Transport agreements RT.2.08 and RT.3.03 (Reamer, 2000a,b), results from this report and the followup report on CNWRA gravity and magnetic studies in the region may be useful toward addressing these agreements.

Included in the suite of surveys were induced polarization, electromagnetic, and Schlumberger D.C. electrical resistivity studies designed to delineate the near-surface electrical resistivity structure of the region. The near-surface electrical resistivity structure is expected to reflect the near-surface geology and hydrogeology, including the transition from the unsaturated to the saturated zone.

An initial survey was planned and executed in 1998 prior to the initiation of the Nye County Early Warning Drilling Program. The goal of this early survey was to evaluate the applicability of the time-domain electromagnetic method to support delineation of the major hydrogeologic and geologic features of the region in a noninvasive and cost effective manner. Following preliminary assessments from this initial survey (Sandberg, 1998a), several other surveys that included additional geophysical techniques were planned and subsequently executed in 1999. Where possible, the locations of these surveys were selected to coincide with well placements proposed by the Nye County Early Warning Drilling Program. This chapter summarizes these methods, their deployment in southern Fortymile Wash and northern Amargosa Valley, and subsurface models of the geology and hydrogeology developed based on the data collected. It should be noted the discussions provided in this chapter enhance the discussions and models contained in the data processing and interpretation reports of Sandberg (1998a, 2000).

3.1 Summary of the Methods Applied

Schlumberger D.C. electrical resistivity, induced polarization, and time-domain electromagnetic resistivity depth-sounding methods constituted the suite of measurements performed. This suite

of methods has been shown in the past to provide constraints for subsurface models when used in a simultaneous inversion modeling framework (Sandberg, 1993). Although the application of this suite of measurements at each sounding station is ideal for characterization, time constraints dictated the entire suite be applied only at selected locations. Hence, at some sounding stations, only one method, time-domain electromagnetic resistivity depth sounding, was used. This choice was dictated by the greater depth of penetration capable with this method compared with the other survey methods in the suite.

3.1.1 Schlumberger D.C. Electrical Resistivity Depth-Sounding Method

The Schlumberger D.C. electrical resistivity depth-sounding array (Figure 3-1) consists of two electrodes (A and B) for injecting electrical current into the ground and two additional electrodes (M and N) for recording the resulting electrical potential differences between two points at the ground surface. These measurements are often reduced to apparent electrical resistivities *(ρ_a)* using (based on Sandberg, 1998b, Eq. 21)

$$\rho_a = \frac{\pi \Delta V}{2 I I} (L^2 - l^2) \tag{3-1}$$

where

L	—	half the distance between the current electrodes A and B
l	—	half the distance between electrodes M and N
I	—	the magnitude of the injected electrical current at A and B
ΔV	—	the measured potential difference between M and N

Apparent resistivity is generally not a correct estimate of the subsurface electrical resistivity distribution. Rather, it represents the electrical resistivity of a uniform homogeneous medium that would produce the observed potential difference given the injected current and the geometric configuration of the electrodes. Hence, the apparent electrical resistivity only reflects the true electrical resistivity of the subsurface for homogeneous or mildly heterogeneous conditions. For the Schlumberger D.C. electrical resistivity depth-sounding data, one-dimensional heterogeneous models of the subsurface electrical resistivity may be constructed using geophysical inversion techniques. These techniques will be discussed later in this report.

3.1.2 Induced Polarization Method

Induced polarization describes the electrical potential decay phenomenon observed after a direct current injected into the surface is instantaneously turned off. After the injected current is discontinued, the measured potential difference is observed to gradually decay to zero. The voltage decay, measured as a function of time, is referred to as time-domain induced polarization.

There are two mechanisms identified as the source for induced polarization: membrane polarization and electrode polarization. Membrane polarization results from a nonequilibrium

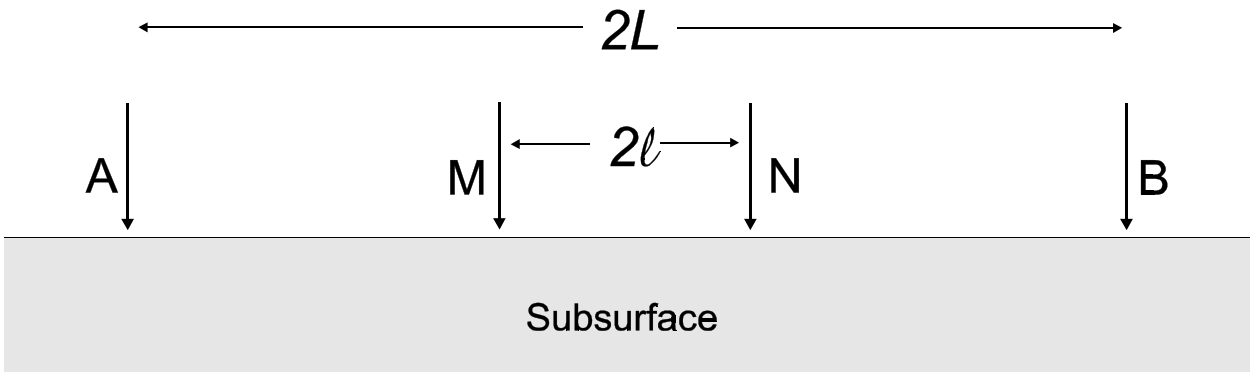

Figure 3-1. Schematic of Schlumberger D.C. Electrical Resistivity Depth-Sounding Array

distribution of ions in pore fluids in an applied voltage and is enhanced by the presence of charged mineral and soil grains, including clay particles. After current flow is induced through a medium in which ions are uniformly distributed, the motion of negatively charged ions may be inhibited by the presence of negatively charged minerals and soil grains. This inhibition results in localized regions of negative ion accumulation. Discontinuing the induced current flow produces a measurable voltage decay as ions diffuse away from zones of accumulation to reestablish a uniform distribution.

Electrode polarization is caused by the presence of conductive minerals in the subsurface. When these minerals are present, electrical current flow is by electronic conduction. This leads to an accumulation of ions at the interface between the mineral and solution, resulting in an increase in the electrochemical voltage at the metallic grain surfaces. After the applied external voltage is discontinued, the electrochemical voltage decays with time. The rate of voltage decay is proportional to the concentration of metallic minerals in the rock.

Clay-rich units are known to exist within the valley-fill deposits in Fortymile Wash and northern Amargosa Valley as demonstrated by geologic logs recorded at several Nye County Early Warning Drilling Program Wells (e.g., Well 5S). These clay-rich units can be expected to contribute to membrane polarization and, hence, induced polarization. Also present in Fortymile Wash and northern Amargosa Valley are geologic units that represent intact and weathered volcanic units. These units may support the induced polarization effect. The significance of this contribution, however, is not clear because of uncertainties related to the size and spatial continuity of these volcanic units.

The physical property often estimated in induced polarization surveys is chargeability. This property provides an indication of the electrical capacitance of the subsurface and reflects the time required for the polarization effect to decay to background conditions. Several approaches exist for estimating chargeability, however, the expression commonly used and integrated into most commercial time-domain induced polarization equipment is (Sharma, 1997)

$$M = \frac{1}{V_0}\int_{t_1}^{t_2} V(t)\,\mathrm{d}t \qquad (3\text{-}2)$$

where

M	—	chargeability
V_0	—	voltage at cutoff
$V(t)$	—	voltage as a function of time during the decay cycle
t	—	time

3.1.3 Time-Domain Electromagnetic Method

The time-domain electromagnetic resistivity depth-sounding method is a broadband electromagnetic technique (Sandberg, 2000) in which current is rapidly turned off in a surface transmitter wire loop after a steady-state magnetic field has been created. In accordance with Faraday's Law, the changing magnetic field associated with the decaying current induces a changing current flow in subsurface conductors. The decay of the secondary magnetic field associated with the variable current flow induced in the subsurface can be recorded at the surface using a wire coil. By analyzing the primary and secondary magnetic fields, a model of the subsurface can be developed.

Several time-domain electromagnetic measurement configurations are possible. The most often used configuration, and the simplest to apply, is the central loop depth-sounding configuration. This configuration consists of a large square transmitter loop laid out at the ground surface. At the center of the transmitter loop is a much smaller receiver coil. Data from this configuration are commonly interpreted using a one-dimensional model. Assumptions inherent in this model are that electrical resistivity layers are horizontal and laterally continuous, layer electrical resistivities are homogeneous, and the electrical resistivity within each layer is isotropic.

Although time-domain electromagnetic resistivity depth-sounding data can be inverted on their own, they are insensitive to near-surface changes and to highly resistive layers, even when the latter are quite thick (Sharma, 1997). To overcome this limitation, joint inversion of time-domain electromagnetic and Schlumberger D.C. electrical resistivity depth-sounding data is sometimes used, with the latter providing strong constraints on the near-surface interpretation. From a hydrogeologic perspective, however, none of these methods is well suited to differentiating high electrical conductivity clay layers in the subsurface from water saturated formations. For this reason, inclusion of induced polarization data within the joint inversion framework is compelling.

As with most electrical resistivity methods, apparent resistivity is readily computed by the measuring instrument. For time-domain electromagnetic resistivity depth-sounding instruments, the field-based apparent resistivity is often expressed as a function of time, either early time or late time. Here, the measured response at early time is largely from the near-surface layers, whereas, the late-time response is predominantly from lower layers. Because characterization of the deeper structures is important for this work, greater emphasis is placed on modeling the late-time data.

In the analyses of the field data collected in this work, apparent resistivities were calculated using two methods. The first analysis approach is based on the late-time asymptotic relationship (Sandberg, 1998b)

$$\rho_a = \frac{a^{4/3} A_R^{2/3} \mu_0^{5/3}}{20^{2/3} \pi^{1/3} t^{5/3} Z^{2/3}} \tag{3-3}$$

where

a	—	radius of an equivalent circular transmitter loop
A_R	—	area of the receiver coil
$\mu_0 = 4\pi \times 10^{-7}$	—	magnetic permeability of free space
t	—	sample time
Z	—	receiver voltage divided by the transmitter current

The first approach assumes a step function transmitter turnoff and is only accurate at late times.

The second method uses a ramp-correction that accounts for the finite transmitter turn-off ramp (Sandberg, 1998b). This approach is reasonably accurate for determining the near-surface or early-time resistivity structure. Ramp-corrected, time-based apparent resistivities are converted to depth-based approximate resistivities using Meju (1998, Eq. 2)

$$\delta_{\text{eff}} = \sqrt{\frac{3.9 \rho_a t}{2\pi\mu_0}} \tag{3-4}$$

where δ_{eff} represents effective depth.

3.2 Data Modeling

Recognizing the limitations inherent in modeling geophysical data, simultaneous-inverse modeling of collected data was applied when multiple data sets were available. The inclusion of multiple geophysical data sets in the simultaneous-inversion framework minimizes model nonuniqueness through the implicit inclusion of additional model constraints.

Two approaches to one-dimensional modeling exist: approximate analysis, often referred to as imaging, and discrete-layer modeling. In the latter, the zones of discrete electrical resistivity are assumed independent. This assumption can produce significant discontinuities in the electrical resistivity field and is appropriate for modeling environments in which sharp electrical resistivity transitions occur. In the imaging process, the electrical resistivity is modeled as a continuous function. Where sharp electrical resistivity discontinuities exist, this approach can smear the interface. EINVRT6 (Sandberg, 1998b), the computer code used to perform the single and simultaneous-inversions documented in this work, is based on the discrete layer modeling framework.

EINVRT6 (Sandberg, 1998b) supports inversion of Schlumberger D.C. electrical resistivity depth-sounding, induced polarization, and time-domain electromagnetic data sets either separately or jointly: (i) D.C. electrical resistivity and induced polarization data, (ii) D.C. electrical resistivity and time-domain electromagnetic data, and (iii) D.C. electrical resistivity, induced polarization, and electromagnetic data. Parameter values derived from the inversion include layer electrical resistivity and thickness. The conceptual and mathematical approximations used in this software are summarized in Sandberg (1998b) and are not reproduced in this report.

As noted earlier, a common problem associated with the inversion of geophysical data is model nonuniqueness. Here, nonuniqueness refers to the fact that several geological configurations can produce similar geophysical responses at the location of the recording device. Although all these configurations may be mathematically plausible, some may be unrealistic given the geologic history of the site. Although the simultaneous inversion of multiple data sets in EINVRT6 (Sandberg, 1998b) constrains the range of plausible mathematical and geological models that fit the data, it does not completely eliminate nonuniqueness. Hence, model nonuniqueness can, in some cases, support the identification of alternate conceptual models, where alternate conceptual models represent the range of plausible geological models and not the total number of alternate mathematical models that result from the inversion process. This version of an alternate conceptual model differs from alternate conceptual models that may result from uncertainties associated with the interpolation of sparse point data.

The cross-sectional models presented in this report are based on one-dimensional geophysical inversion and spacial correlation and should be viewed as drawn from a list of alternate conceptual models. Where possible, these models are verified through comparisons with available field data. Future verification with additional geophysical models will be provided in a subsequent report.

3.3 Field Surveys and Modeling Results

The locations of the 1998 and 1999 geophysical surveys in southern Fortymile Wash and northern Amargosa Valley are shown in Figure 3-2. Preliminary modeling and interpretation of the 1998 and 1999 data are summarized in Sandberg (2000, 1998a). This section summarizes the surveys performed and resulting electrical resistivity cross-sectional models produced by combining the one-dimensional models developed through geophysical inversion for the various sounding stations.

3.3.1 1998 Time-Domain Electromagnetic Resistivity Depth-Sounding Field Survey

The time-domain electromagnetic resistivity soundings that constitute the 1998 survey were performed to investigate the adequacy of the time-domain electromagnetic method to characterize the hydrogeology and geology of southern Fortymile Wash and northern Amargosa Valley. In particular, the survey was aimed at filling the greater than 10-km [6.2-m] hydrogeological data gap that extends from Well JF–3 in the north to the community of Amargosa Farms in the south.

The survey is composed of 10 sounding locations [Figure 3-2 (Transect F-F') and Appendix (Table 1a)] occupied during spring 1998. To effectively image the anticipated depth of the water table, 200 × 200-m [656 × 656-ft] and 60 × 60-m [197 × 197-ft] transmitter loops were used with applied signal frequencies of 32 and 8 Hz. Sandberg (1998a) describes the data quality along

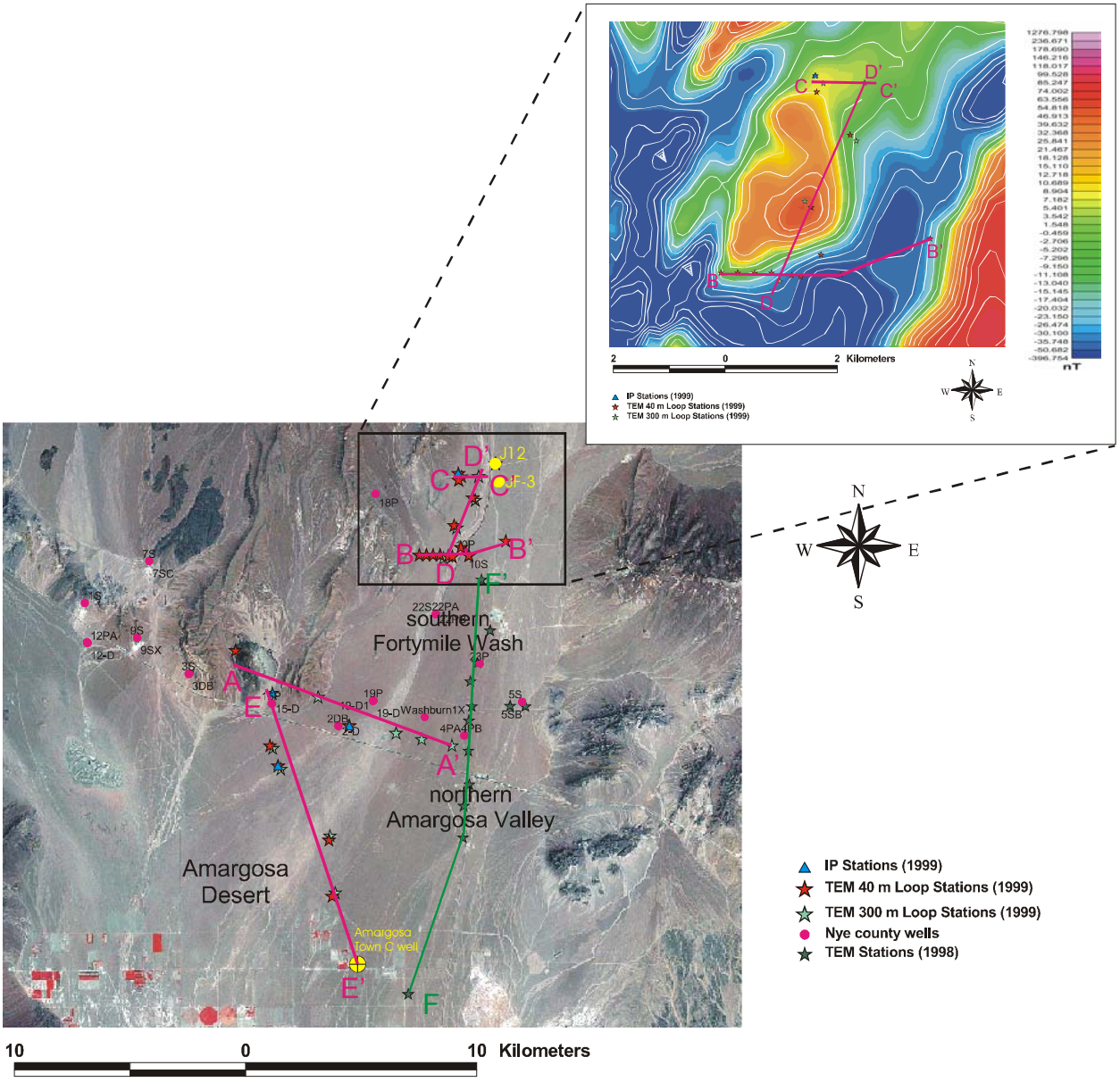

Figure 3-2. Locations of Schlumberger D.C. Electrical Resistivity Depth Soundings, Time-Domain Electromagnetic (TEM) Resistivity Depth Soundings, and Induced Polarization (IP) Depth Soundings. Inset Figure Shows the Transects B-B', C-C', and D-D' Superimposed on a Portion of an Aeromagnetic Map Based on Blakely, et al., 2000. NOTE: Scale information provided in kilometers; for conversion use 1 km = 0.621 m.

this transect as good, with the exception of data from station D (not shown on the transect) where the 32- and 8-Hz apparent electrical resistivity data do not overlap from 0.00006 to 0.0006 seconds. Data collected at each of the remaining sounding stations were modeled using EINVRT6 (Sandberg, 1998b) and an assumed four-layer model to produce a series of discrete electrical resistivity layers and associated thicknesses (Figure 3-3). Note that

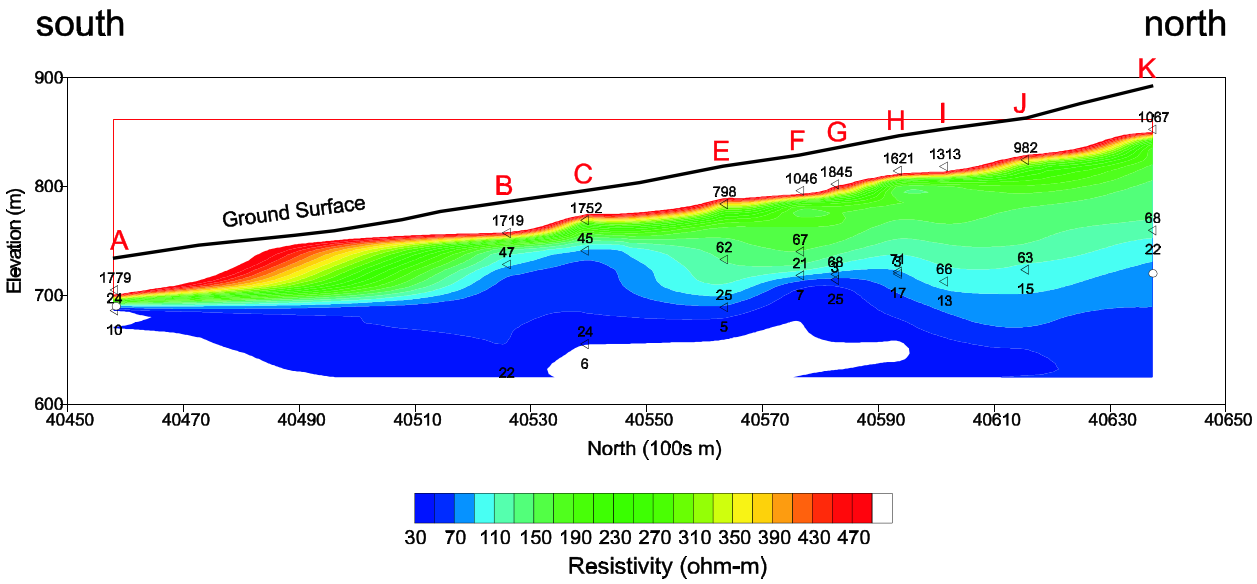

Figure 3-3. Electrical Cross Section for 1998 Survey Transect F-F' (see Figure 3-2). Numbers on the Figure Represent Electrical Resistivities in ohm-m. NOTE: Scale information provided in meters; for conversion use 1 m = 3.281 ft.

Figure 3-3 also contains a contoured plot of the computed apparent electrical resistivity depth section [see Eqs. (3-3) and (3-4)] for the transect.

The upper layer of each model is 25 to 40 m [82 to 131 ft] thick and is characterized by a high electrical resistivity that commonly exceeds 1,000 ohm-m. These electrical resistivities are consistent with those reported by Greenhaus and Zablocki (1982) based on their modeling effort and are significantly greater than those of the underlying layer. These high electrical resistivities likely reflect hydrologic and lithologic variations within the near surface. The modeled magnitude and thickness of the layer at each station, however, may be affected by modeling nonuniqueness, even though this effect is expected to be reduced by the simultaneous inversion of the 32- and 8-Hz data.

The transition from the upper layer to the underlying lower electrical resistivity layer is abrupt. Modeled electrical resistivities in the underlying layer range from 45 to 75 ohm-m. As mentioned before, the modeled transition may result from a combination of lithologic and hydrologic factors. Lithologic logs from Nye County Early Warning Drilling Program Wells 4PA and 4PB (not shown on Figure 3-4), which are in close proximity to sounding station E (Figure 3-4), do not appear to show the modeled transition. Soil moisture logs recorded at these Nye County Early Warning Drilling Program wells also do not appear to support the modeled transition. It should be noted, however, the soil moisture logs reported for the Nye County Early Warning Drilling Program wells were recorded several years after the geophysical surveys were completed and, because of the transient nature of soil moisture, may not represent previous field conditions at the time of the surveys. Unfortunately, few geophysical logs are available at the current time for the Nye County Early Warning Drilling Wells 4PA and 4PB.

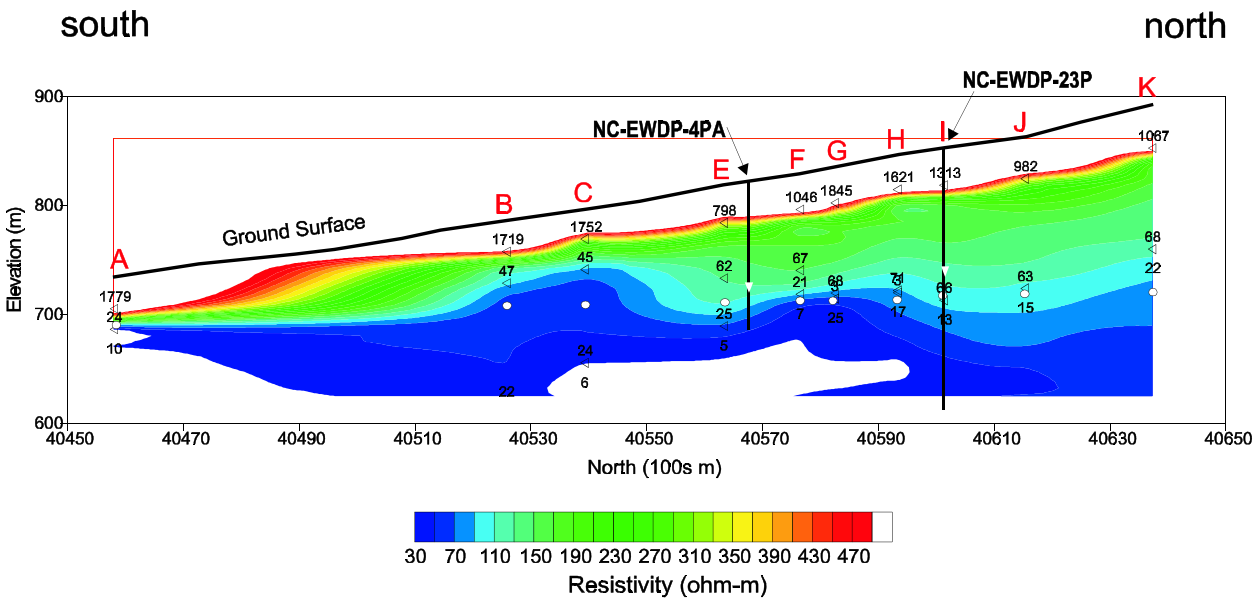

Figure 3-4. Comparison of Data from Nye County Early Warning Drilling Program Wells (NC–EWDP) 4PA and 23P and Hill, et al. (2002) to the Electrical Cross Section for 1998 Survey Transect F-F'. White Dots Represent Water Table Elevation Estimates from Hill, et al. (2002), and White Triangles Represent Water Table Elevation Estimates from Nye County Early Warning Drilling Program Wells. NOTE: Information provided in meters; for conversion use 1 m = 3.281 ft.

Available well logs for Nye County Early Warning Drilling Program Well 23P (which is in close proximity to sounding station I) also were reviewed in an effort to further explore the cause of the first transition. Unfortunately, no lithologic logs currently are available for this well, and available electrical resistivity logs do not cover the depth of interest. A comparison of the modeled electrical resistivity profile with the magnetic logs at the depth of the transition shows a possible correlation (Figure 3-5). It is important to note the trend in the magnetic logs shows good correlation to the trend in the caliper log. Whether these correlations are indicative of lithologic variations in the region will be investigated in a followup report once a comprehensive set of lithologic and geophysical logs for the Nye County Early Warning Drilling Program Wells 4PA, 4PB, and 23P becomes available.

The second transition modeled separates electrical resistivities of 45–70 ohm-m of the second layer from underlying third layer electrical resistivities of 7–25 ohm-m. The electrical resistivities in the third layer zone are interpreted to reflect the regional aquifer system. To investigate this assumption, the measured depths to the water table at the Nye County Early Warning Drilling Program Wells 4PA and 23P were superimposed on the electrical resistivity section for transect F-F' (see Figure 3-4). The comparison shows the elevation of the measured water table is generally within 10–20 m [33–66 ft] of the modeled interface between the second and third layers and, therefore, appears to support the assumption. The assumption is further supported by the general agreement between the elevation of the interface and the water table elevations extracted from the contour map of Hill, et al. (2002). These differences may be due to the combined effects of modeling nonuniqueness and model resolution. The area of poor stations B and C where a low electrical resistivity mound is modeled and also reflected in the apparent electrical resistivity depth section (Figures 3-3 and 3-4). These soundings appear to

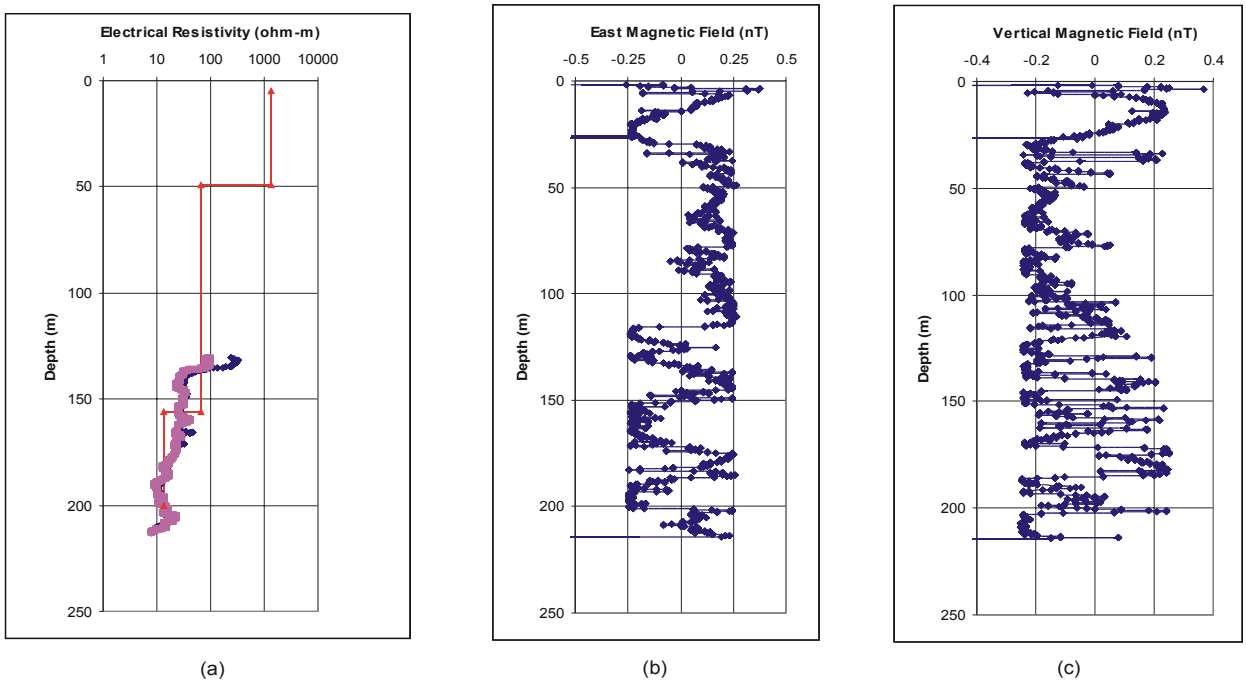

Figure 3-5. Comparison of Modeled Electrical Resistivities at Sounding Station I (Transect F-F') to Geophysical Logs from Nye County Early Warning Drilling Program Well 23P: (a) Modeled Electrical Resistivities (Orange), R16 Resistivity Log (Pink), and R64 Resistivity Log (Navy Blue); (b) East Component of Magnetic Log; and (c) Vertical Component of Magnetic Log
NOTE: Information provided in meters; for conversion use 1 m = 3.281 ft.

coincide with the location of the buried volcanic cone Magnetic Anomaly B (Figure 3-6). Depths agreement between the modeled transition and the map of Hill, et al. (2002) occurs at sounding to the second interface at sounding stations B and C compare favorably to the observed depths to the tuff/valley-fill interface {61–73 m [200–240 ft]} reported for the Felderhoff wells by Carr, et al. (1995). Figure 3-6 also shows the magnetic anomalies that result from the complicated distribution of tuff and basalt units along the transect.

3.3.2 1999 Resistivity Field Surveys

In 1999, a suite of time-domain electromagnetic and Schlumberger D.C. electrical resistivity depth soundings, as well as induced polarization soundings, was designed and executed to address the hydrologic data gaps that existed in the region prior to development of the Nye County Early Warning Drilling Program. Although the Nye County Early Warning Drilling Program wells have increased the amount of data available for this region and further constrained the geology of the area, the geophysical soundings performed in 1999 remain important because they provide a means through which hydrostratigraphies and the water table may be spatially mapped in interwell regions.

The 1999 field survey consisted of 35 time-domain electromagnetic resistivity depth soundings, 4 time-domain induced polarization depth soundings, and 4 Schlumberger D.C. electrical resistivity depth soundings (Figure 3-2). For the time-domain electromagnetic resistivity depth soundings, two rectangular transmitter loop sizes {300 × 300 m [984 × 984 ft], and 40 × 40 m

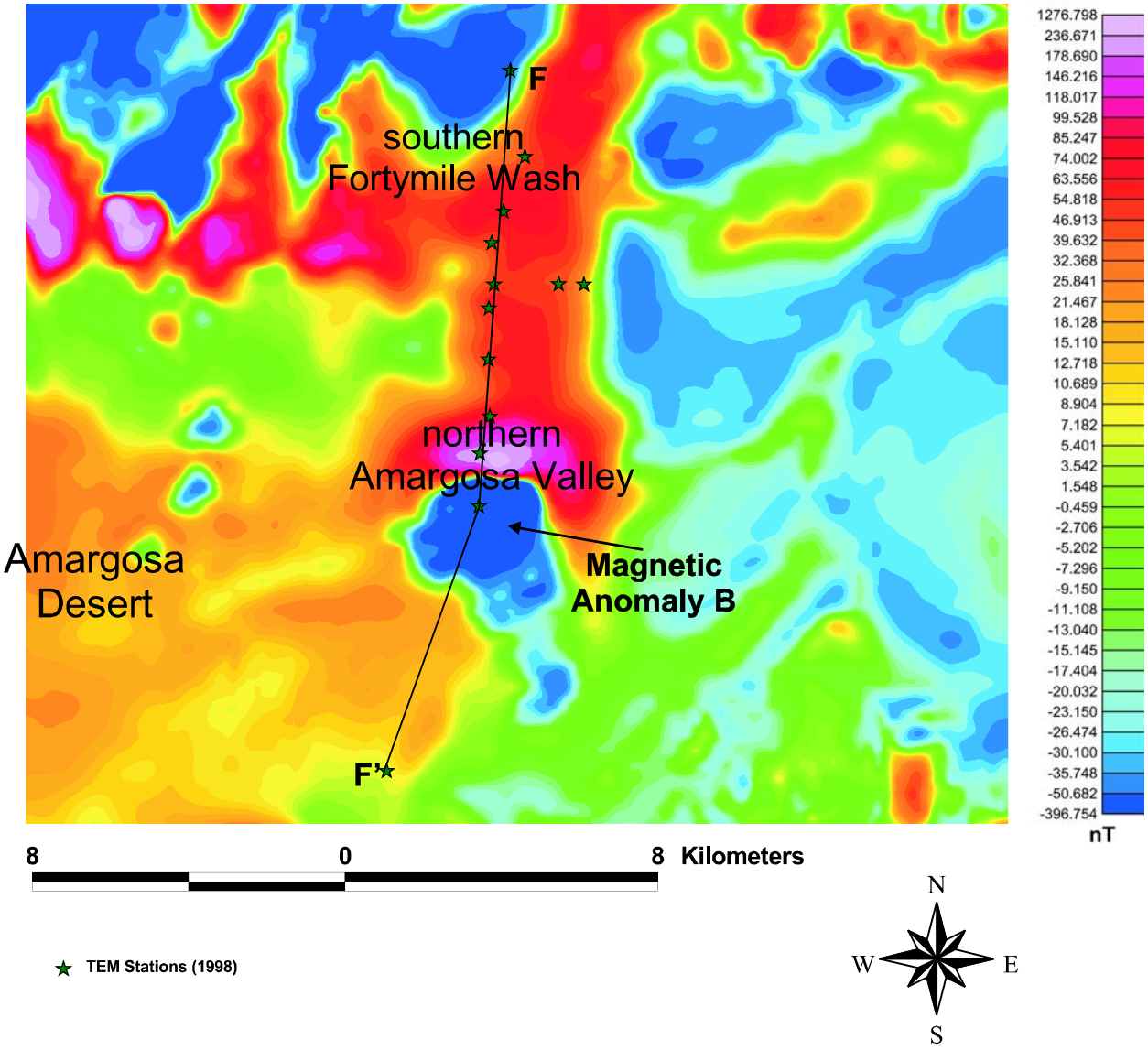

Figure 3-6. Distribution of Aeromagnetic Magnetic Features (Based on Blakely, et al., 2000) Relative to Transect F-F'.
NOTE: Scale information provided in meters; for conversion use 1 m = 3.281 ft.

[131 × 131 ft]} and several transmitter frequencies (3, 30, 75, and 285 Hz) were used to map both near-surface and deeper resistivity features. As the time-domain induced polarization and Schlumberger D.C. electrical resistivity depth soundings were much more time consuming than the time-domain electromagnetic soundings and only constrained the near-surface environment, only four of each of these two soundings were performed (Figure 3-2).

Five transects (resistivity depth sections) were constructed from the suite of measurements, A-A', B-B', C-C', D-D', and E-E' as shown in Figure 3-2. Line A-A' extends across southern

Fortymile Wash and was constrained by data at Nye County Early Warning Drilling Program Wells 15P, 2D, Washburn 1X, and 4PB (see Figure 3-2). Note that prior to development of Nye County Early Warning Drilling Program Well 15P, Farrell, et al. (2000) used data from a well located at the Lathrop Wells cinder cone to constrain interpretation of the western portion of Line A-A'. Lines B-B', D-D', and C-C' intersect each other and are located on the Nevada Test Site, west of the Fortymile Wash channel. Few data exist to constrain the models along these lines. Hence, an attempt was made to constrain the interpretation of the station models and resulting electrical resistivity cross section with data from Wells JF–3, J–13, J–12, and Nye County Early Warning Drilling Program Well 10S. Line E-E' extends from the Lathrop Wells cinder cone toward Amargosa Farms and, as a result, crosses the central portion of the Amargosa Desert. The interpretation of this line is constrained using data from Nye County Early Warning Drilling Program Well 15P and the Amargosa Farms Town C Well.

3.3.2.1 Transect A-A'

Electrical resistivity and chargeability models determined from the single and simultaneous inversions of data sets recorded at stations along transect A-A' were used to construct the cross section shown in Figure 3-7. Along this line, models based on simultaneous inversion of multiple data sets were considered the most reliable based in part on the ranges of the 95-percent confidence intervals estimated for inverted parameters (Farrell, 2000; Sandberg, 2000). The computed one-dimensional models and resulting cross section show the subsurface electrical resistivity structure to be vertically layered and laterally correlated. That is, electrical resistivity contacts can be reasonably correlated across sounding stations.

The electrical resistivity cross section is made up of two major layers, an upper layer of relatively high electrical resistivity and an underlying layer of lower electrical resistivity. Additional electrical resistivity layering can be inferred within these primary layers. The general distribution of electrical resistivities is similar to that shown in Figure 3-3. Electrical resistivities in the upper layer generally exceed 80 ohm-m and at shallow depth may locally exceed 500 ohm-m. In contrast, electrical resistivities in the lower layer are generally less than 25 ohm-m, with exceptions occurring at sounding locations TEM-2 and TEM-1. The greater than 600-ohm-m electrical resistivity modeled at TEM-2 is suspect and assumed to reflect model nonuniqueness. This assumption is supported by a similarly modeled feature at TEM-1 when the inversion is based solely on time-domain electromagnetic resistivity data (Table 3-1). When Schlumberger D.C. electrical resistivity depth-sounding and induced polarization data are simultaneously included in the inversion at TEM-1 (Figure 3-7), the magnitude of this feature is noticeably reduced to approximately 132 ohm-m. Although the magnitude of the electrical resistivity of the zone is noticeably reduced, the zone remains electrically resistive relative to adjacent zones.

The magnitude of the observed high electrical resistivity zone that approaches the ground surface at TEM-4 is significantly greater than that observed at other stations along the transect. Although the magnitude of the electrical resistivity of this zone may be due in part to model nonuniqueness, it is assumed the large magnitude is reflective of subsurface conditions in the vicinity of the measurement. Note that TEM-4 is located immediately west of the Lathrop Wells cinder cone in an area dominated by volcanic units that crop out at the ground surface. Currently, it is assumed the high electrical resistivity zone reflects dry conditions in these units. The overlying lower electrical resistivity zone may reflect a mixture of volcanic clasts and moist valley-fill sediments.

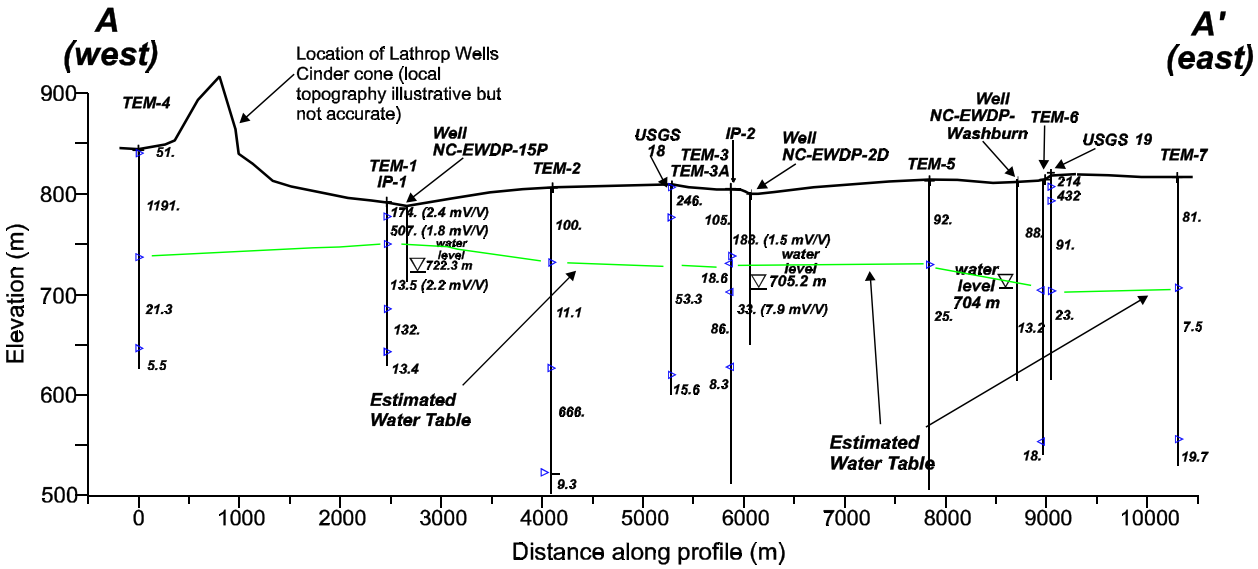

Figure 3-7. Electrical Cross Section for Transect A-A' (See Figure 3-2). Numbers in Parentheses on the Figure Represent Chargeabilities in mV/V and Numbers without Parentheses Represent Electrical Resistivities in ohm-m. NC–EWDP Represents Nye County Early Warning Drilling Program.
NOTE: Information provided in meters; for conversion use 1 m = 3.281 ft.

Table 3-1. Electrical Resistivity Model for Station TEM-1 Based on Inversion of Time-Domain Electromagnetic Resistivity Depth-Sounding Data		
Layer	**Electrical Resistivity (ohm-m)**	**Thickness (m)**
1	434.0	41.8 [137.1 ft]
2	13.4	67.3 220.8 ft]
3	656.6	38.0 [124.8 ft]
4	13.4	—

In an effort to validate the modeling results, models developed for the region that includes TEM-3, TEM3-A, and IP-2 were compared with gamma and electrical resistivity logs recorded at Nye County Early Warning Drilling Program Well 2DB (Figure 3-8), which is in close proximity to Nye County Early Warning Drilling Program Well 2D. The inverted electrical resistivity models correlate reasonably well with the general trends in the electrical resistivity logs with deviations occurring at depth. These deviations are because of the combined decreasing resolution of the surveying methods with depth as well as the number of layers and associated constraints specified in the starting models of the inversion process.

To further validate the models associated with this cross section and the cross section developed for transect F-F', a comparison with the models developed for TEM-7 and the nearby TEM station E on transect F-F' was performed. The upper contact modeled at station E is not

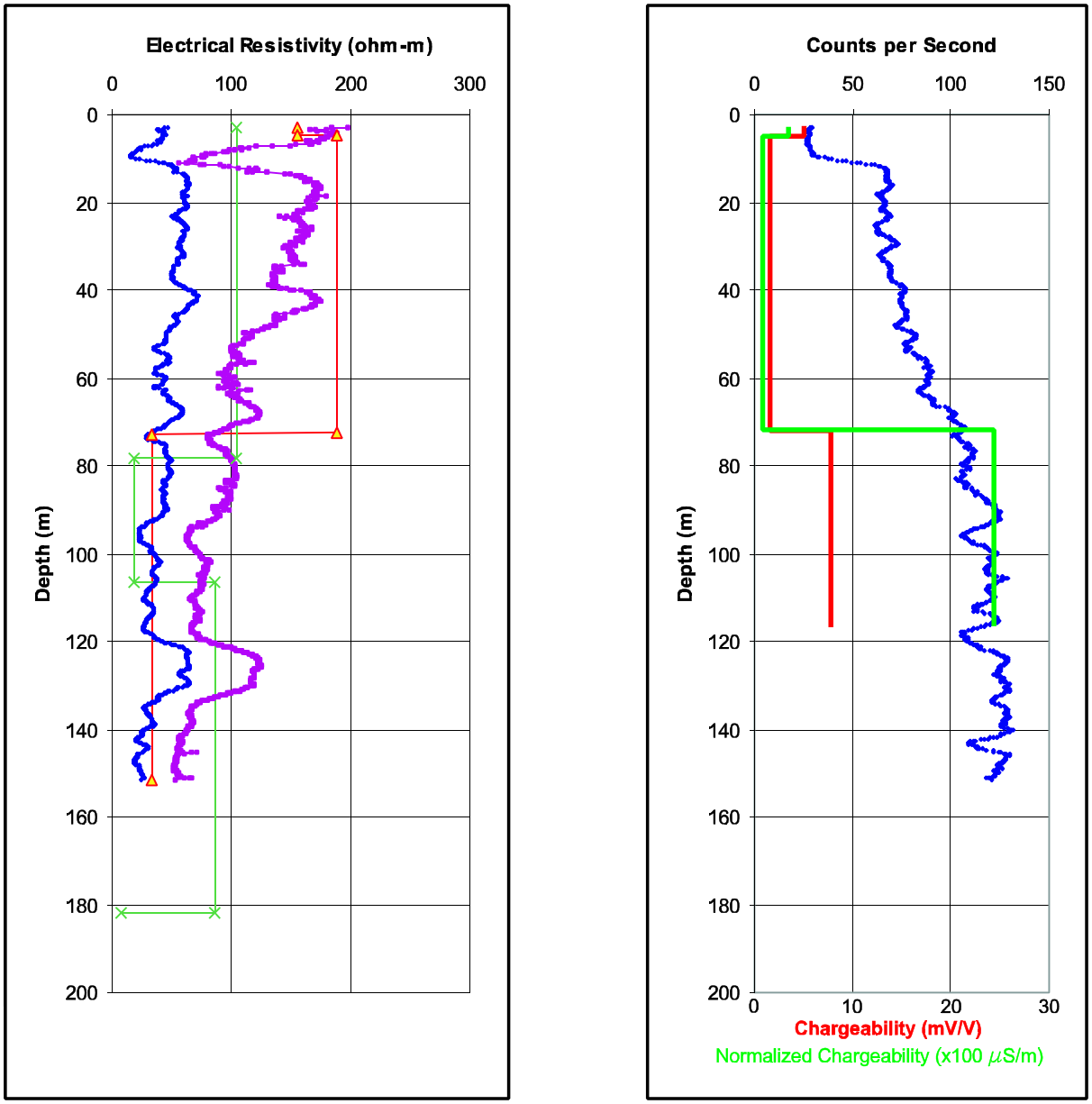

Figure 3-8. Comparison of Electrical Resistivities Modeled at TEM-3/TEM-3A and IP-2 with Logs for Nye County Early Warning Drilling Program Well 2DB: (a) R64 Resistivity Log (Purple), R16 Resistivity Log (Navy Blue), IP-2/Schlumberger Simultaneous Inversion Model (Red), TEM-3/TEM-3A Simultaneous Inversion Model (Green); (b) Gamma Log (Navy Blue), Modeled Chargeability (Red), Normalized Chargeability (Green) NOTE: Information provided in meters; for conversion use 1 m = 3.281 ft.

modeled at TEM-7. This is because only 300 × 300-m [984 × 984-ft] loop low frequency data were collected at TEM-7 and, as a result, near surface features are not well resolved. Recall that the model developed for station E was based on the simultaneous inversion of 60 × 60-m [197 × 197-ft] and 200 × 200-m [656 × 656-ft] data that supported resolution of this feature. It should be noted that TEM-1/IP-2 shows the presence of this high resistivity unit along transect A-A'. The second contact modeled at station E shows a transition from high electrical resistivity (62 ohm-m) to lower electrical resistivity (25 ohm-m). The elevation of this transition shows reasonable correlation to transition from high electrical resistivity (81 ohm-m) to low electrical resistivity (7.5 ohm-m) at sounding location TEM-7. Differences in elevations of the two transitions may be because of modeling uniqueness, modeling assumptions, and local variations in geology.

Chargeabilities inverted from the induced polarization data also show good correlation to the gamma log for the Nye County Early Warning Drilling Well 2D. This correlation is assumed to reflect the increased clay content with depth described in the geologic log. Note the correlation of the induced polarization model with clay content can be enhanced using the normalized chargeability (Slater and Lesmes, 2002) (chargeability/electrical resistivity) ×100 (Table 3-2) where the larger values indicate higher clay content.

Water table elevations recorded at Nye County Early Warning Drilling Program Wells 2D and Washburn 1X show reasonable correlation to the primary transition from high to low electrical resistivity modeled at TEM-2, TEM-3/TEM-3A (based on associated Schlumberger data), IP-2, TEM-5, TEM-6, and TEM-7 (Figure 3-5). Note although the general trend in the water table is reproduced, estimated depths to the water table at these stations are generally shallower than the measured depth.

Also modeled in this work were Schlumberger D.C. electrical resistivity depth-sounding data from two U.S. Geological Survey stations, USGS 18 and 19 (Greenhaus and Zablocki, 1982). The modeled transition from high to low electrical resistivity at USGS 19 correlates well with the interpolated water table (Figure 3-7). At USGS 18, the correlation of the interpreted water table to the modeled transition from high to low electrical resistivity is poor.

The water level measurement at Nye County Early Warning Drilling Program Well 15P allows the water table to be interpolated and extrapolated west of Nye County Early Warning Drilling Program Well 2D. It should be noted the water table elevation at Nye County Early Warning Drilling Program Well 15P is higher than at Nye County Early Warning Drilling Program Well 2D,

Table 3-2. Electrical Resistivity Model for Station IP-2 Based on Simultaneous Inversion of Induced Polarization and Schlumberger D.C. Depth-Sounding Data

Layer	Electrical Resistivity (ohm-m)	Chargeability (mV/V)	Thickness (m)	Normalized Chargeability (μS/m) × 100
1	832.7	3.0	1.73 [5.6 ft]	0.4
2	156.5	4.9	3.09 [10.2 ft]	3.1
3	188.2	1.5	67.81 [222.4 ft]	0.8
4	33.0	7.9	—	23.8

indicating an eastward component of the hydraulic head gradient. Using water level data from these two wells, the correlation with the transition from high to low electrical resistivity at TEM-2 is reasonable. At TEM-1/IP-1, the estimated water table occurs at a noticeably higher elevation than at Nye County Early Warning Drilling Program Well 15P. However, the trend of increasing water table elevation toward Nye County Early Warning Drilling Program Well 15P appears to be preserved. Although TEM-1/IP-1 reproduces the general trend in the water table elevation, it is possible the model for this station is impacted by subsurface lateral variabilities associated with the shallow basalt units west of the measurement station. The estimated water table elevation at TEM-4 is lower than at TEM-1/IP-1 and more consistent with TEM-2.

The water table elevations estimated from the interpretation of the geophysical soundings were further compared with water table elevations estimated from the water table contour map of Hill, et al. (2002). In most cases, the trends in the water table elevations determined from the geophysical surveys correlate reasonably well with water table elevations inferred from the contour map (Figure 3-9). As with the measured water levels, however, there are differences in elevations between the modeled water table and the water table contour map of Hill, et al. (2002).

Differences between the measured water table elevation and the interpreted elevation may be because of model nonuniqueness, capillary fringe effects, or interpolation error in the Hill, et al. (2002) map and elevation errors. Elevation effects are considered to represent a minor component of the difference. Capillary fringe effects and near saturated conditions in fine-grained sand and silts can diffuse electrical current flows near the water table and produce a shallowing of the water table determined by electrical methods. The capillary fringe effect can be on the order of several meters in fine-grained soils.

3.3.2.2 Transect B-B'

Transect B-B' is an east-west trending profile located several kilometers north of transect A-A' (Figure 3-2). The transect is composed of the following soundings: TEM-24, TEM-23, TEM-22, TEM-21, TEM-20, TEM-25, TEM-26, TEM-11, TEM-10, TEM-9, and TEM-8. These soundings were conducted with 40 × 40-m [131 × 131-ft] transmitter loop sizes, with the exception of TEM-9 and TEM-20, which were conducted with 300 × 300-m [984 × 984-ft] transmitter loop sizes. Neither induced polarization nor Schlumberger D.C. electrical resistivity depth-sounding measurements were collected along this transect, and, hence, no simultaneous inversions were performed. The primary objective of this survey was to map the tuff/valley-fill contact in the region. Because the depth to the water table in this region is greater than 100 m [328 ft] (based on data from Wells J–12 and JF–3), and, therefore, greater than the expected depth of resolution of the 40 × 40-m [131 × 131-ft] transmitter loop size, it is unlikely these soundings support mapping the regional water table, with the possible exception of soundings TEM-9 and TEM-20.

The electrical resistivity cross section developed for transect B-B' by combining the individual one-dimensional models for the various stations is presented in Figure 3-10. Of the five transects modeled in this report, B-B' is considered the least constrained and, hence, most uncertain, partially because of its dependence on single measurements at each station. Nye County Early Warning Drilling Program Well 10S, which is in close proximity to soundings TEM-9 and TEM-10, is used to verify models developed at these stations.

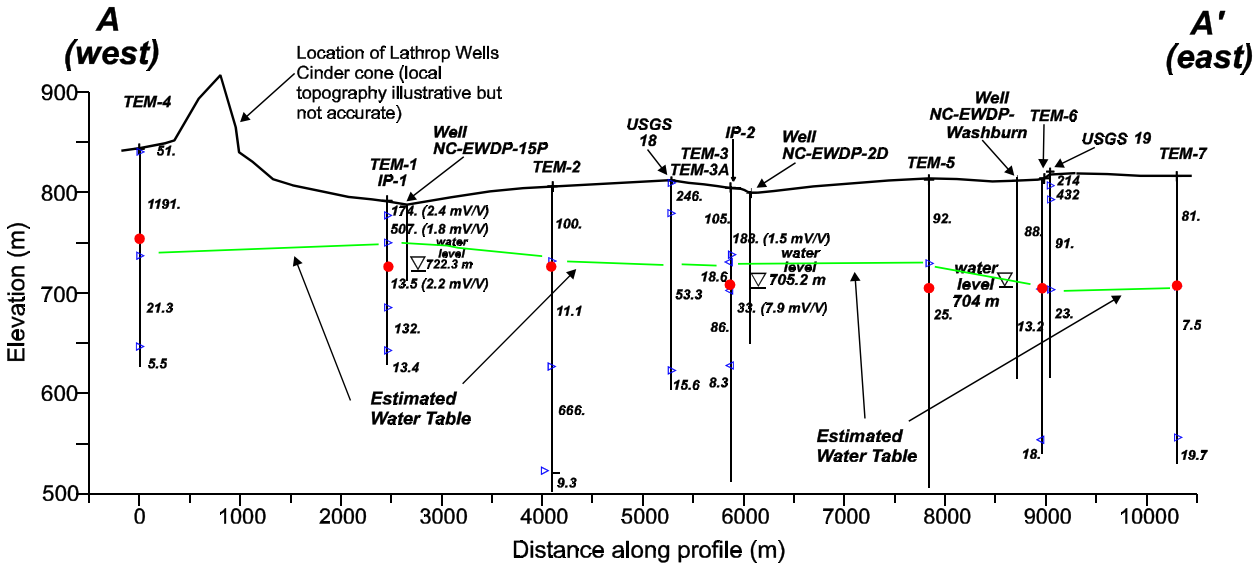

Figure 3-9. Comparison of Estimated Water Table Elevations for Transect A-A' with Estimated Water Table Elevations from Hill, et al. (2002) Represented by Red Dots. Numbers with Parentheses Chargeabilities in mV/V, and Numbers without Parentheses Represent Electrical Resistivities in ohm-m. NC–EWDP Represents Nye County Early Warning Drilling Program.
NOTE: Scale information provided in meters; for conversion use 1 m = 3.281 ft.

The western edge of the B-B' transect is located just east of an eastward dipping tuff outcrop. This known outcrop provides a geological constraint for the one-dimensional models. Because of the proximity of stations TEM-24 and TEM-23 to the east dipping tuff outcrop, there is the possibility the assumption of lateral continuity of geologic units inherent in the one-dimensional modeling may be violated. As a result, there are concerns regarding the accuracy of the one-dimensional electrical resistivity models developed for these two sounding stations. The electrical resistivity models developed for these two stations were found to be the most uncertain, based on the large (orders of magnitude) 95 percent confidence intervals computed for model parameters (Farrell, 2000; Sandberg, 2000).

An initial assessment of transect B-B' indicates differences between the models developed for the 40 × 40-m [131 × 131-ft] transmitter loops and the 300 × 300-m [984 × 984-ft] transmitter loops. Although these different models can lead to alternative conceptualizations for the geology along the transect, it should be realized, the loop sizes and associated sounding frequencies result in differing vertical resolutions and depths of penetrations. These differences, along with the effects of model nonuniqueness, are interpreted to account for the differences between models based on large transmitter loops and small transmitter loops. Transect B-B' displays several shallow layers east of TEM-23. The shallowest layer (not drawn on Figures 3-10 and 3-12, but inferred from station models) is relatively thin and conductive, with modeled electrical resistivities generally less than 50 ohm-m and modeled thicknesses on the order of a few meters. It is important to note this layer is not modeled at TEM-20 and TEM-9, where the use of the large transmitter loop geometry with low frequencies does not

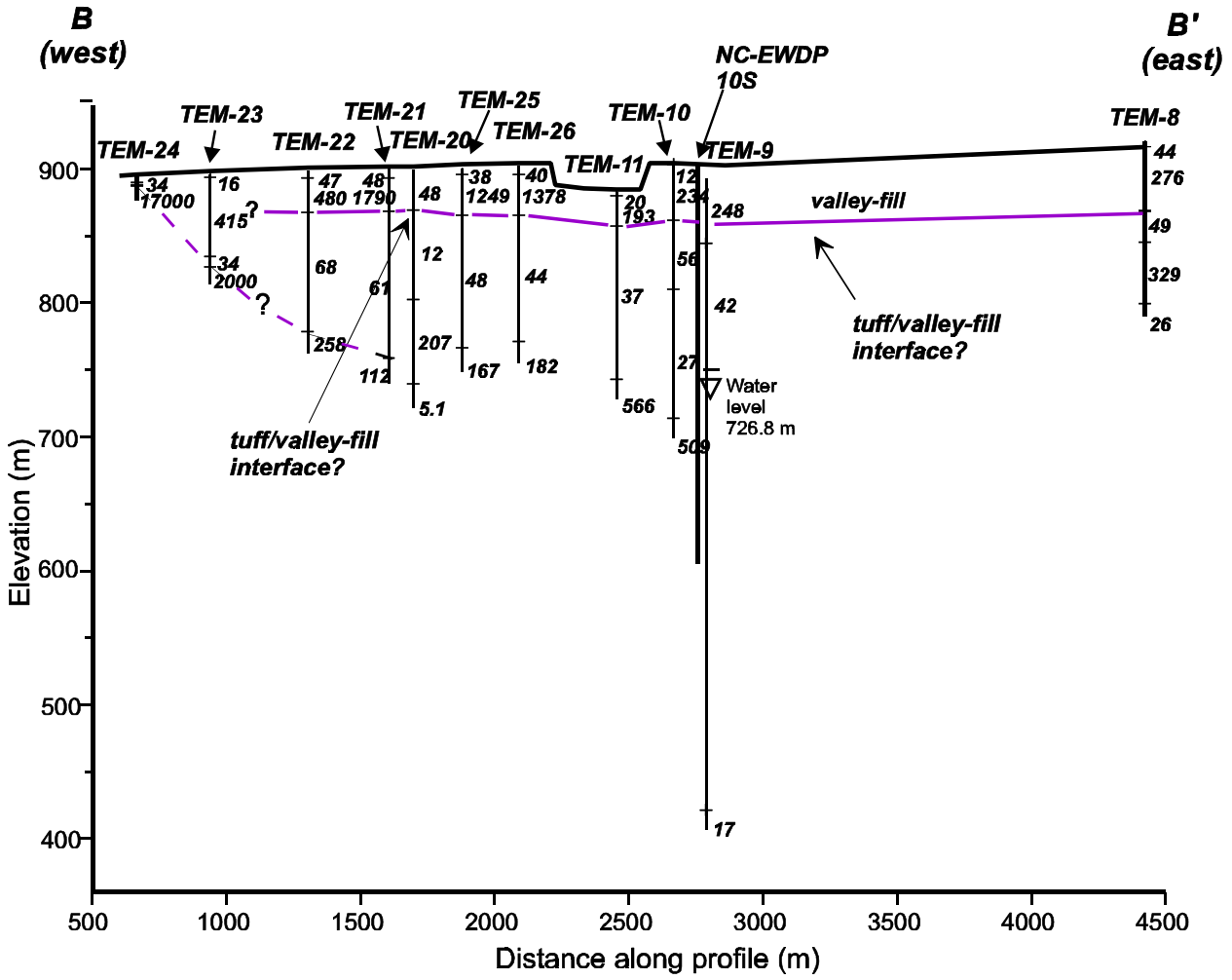

Figure 3-10. Electrical Cross Section for Transect B-B' (see Figure 3-2). Bracketed Numbers Represent Chargeabilities in mV/V, and Numbers without Parentheses Represent Electrical Resistivities in ohm-m. NC–EWDP Represents Nye County Early Warning Drilling Program.
NOTE: Scale information provided in meters; for conversion use 1 m = 3.281 ft.

appear to support its resolution. The low electrical resistivities in this upper zone may reflect either temporal phenomena, such as shallow infiltration following periodic rain events, or a thin conductive clay layer. This surficial layer is underlain by a more electrically resistive unit with modeled electrical resistivities on the order of hundreds to thousands of ohm-m and thickness of tens of meters. This second contact appears to be consistent in elevation with the first modeled contact at TEM-20, but higher in elevation than the first contact modeled at TEM-9. Note the modeled electrical resistivity for the upper layer at TEM-20 is noticeably low compared with adjacent stations and may reflect the limited resolution of this layer.

This layer is, in turn, underlain by a unit of significantly lower electrical resistivity. This transition from high to low electrical resistivity is significantly shallower than the regional water table and more than likely reflects either a change in lithology or a significant increase in the water content

in the valley-fill. Note the thickness of this third layer, which represents the second layer at TEM-20, is thinner at TEM-20 compared with adjacent stations. Although it is possible this difference is because of local structural features, it is more likely this difference reflects the combined effects of model nonuniqueness and reduced resolution, particularly in light of the fact the modeled depth to the base of the third zone is on the order of 2.5 to 3 times the 40 × 40-m [131 × 131-ft] transmitter loop size and, therefore, may be approaching or exceeding the limit of resolution of the measurement configuration. For purposes of completeness, a possible west-dipping contact is illustrated on Figure 3-10 to trace the lower contact of this third layer. Whether this contact represents the tuff/valley-fill contact or whether it represents another transition will be further investigated in a followup report that includes models of magnetic data collected adjacent to the transect.

The models developed for TEM-9 and TEM-10 were compared with electrical resistivity logs recorded at Nye County Early Warning Drilling Program Well 10S (Figure 3-11) to gauge their plausibility. The model developed for TEM-10 reproduces many features observed in the log for Nye County Early Warning Drilling Program Well 105. The model also attempts to reproduce increased electrical resistivity observed at the base of the log. At this depth, the model significantly overpredicts the electrical resistivity. This overprediction is partly because of model nonuniqueness that may be due to the limited resolution of the 40 × 40-m [131 × 131-ft] sounding configuration at this depth. The model developed for TEM-9 likewise reproduces the general trend of the log. The inability of the model to reproduce features in the log reflects the limited number of layers specified in the starting model for the inverse process. Finally, because the electrical resistivity log reflects conditions near the well, including near-borehole effects, it is not expected the log will correlate perfectly with the developed models. Models developed for TEM-10 and TEM-9 were unable to resolve the water table at the Nye County Early Warning Drilling Program Well 10S. Figure 3-12 shows the water table elevations inferred from Hill, et al. (2002) superimposed on the cross section. It is clear that only TEM-20 approximated the water table.

3.3.2.3 Transect C-C'

Transect C-C' trends east-west and is located north of B-B' (Figure 3-2). The transect consists of four time-domain electromagnetic resistivity soundings. At TEM-14 and TEM-13, 40 × 40-m [131 × 131-ft] transmitter loops were used. These two soundings were separated by 260 m [853 ft] and lie along the western side of TEM-12. At TEM-12 and TEM-15, 300 × 300-m [984 × 984-ft] transmitter loops were used. Coincident with TEM-13 is sounding station IP-3. This transect is the shortest of the transects surveyed. Data collected at sounding stations TEM-13 and TEM-14 appeared to be contaminated by either strong lateral inhomogeneities or anthropogenic conductors (e.g., electrical wire) in the near surface and were, therefore, not considered in subsequent analyses. The anomalous behavior observed at sounding stations TEM-13 and TEM-14 was not observed in the data for TEM-12. Because of the proximity of TEM-12 to IP-3, data from these two soundings were combined in a simultaneous inversion. The model uncertainty as determined by the 95-percent confidence intervals for the inverted modeling parameters (Farrell, 2000; Sandberg, 2000) appeared to be moderately constrained. That is, uncertainties for some model parameters appeared to be large (orders of magnitude), whereas for other parameters the uncertainty was small (less than one order of magnitude). The model resolution for TEM-15, however, appeared to be rather poor as determined by the 95-percent confidence intervals for the inverted modeling parameters (Farrell, 2000; Sandberg, 2000).

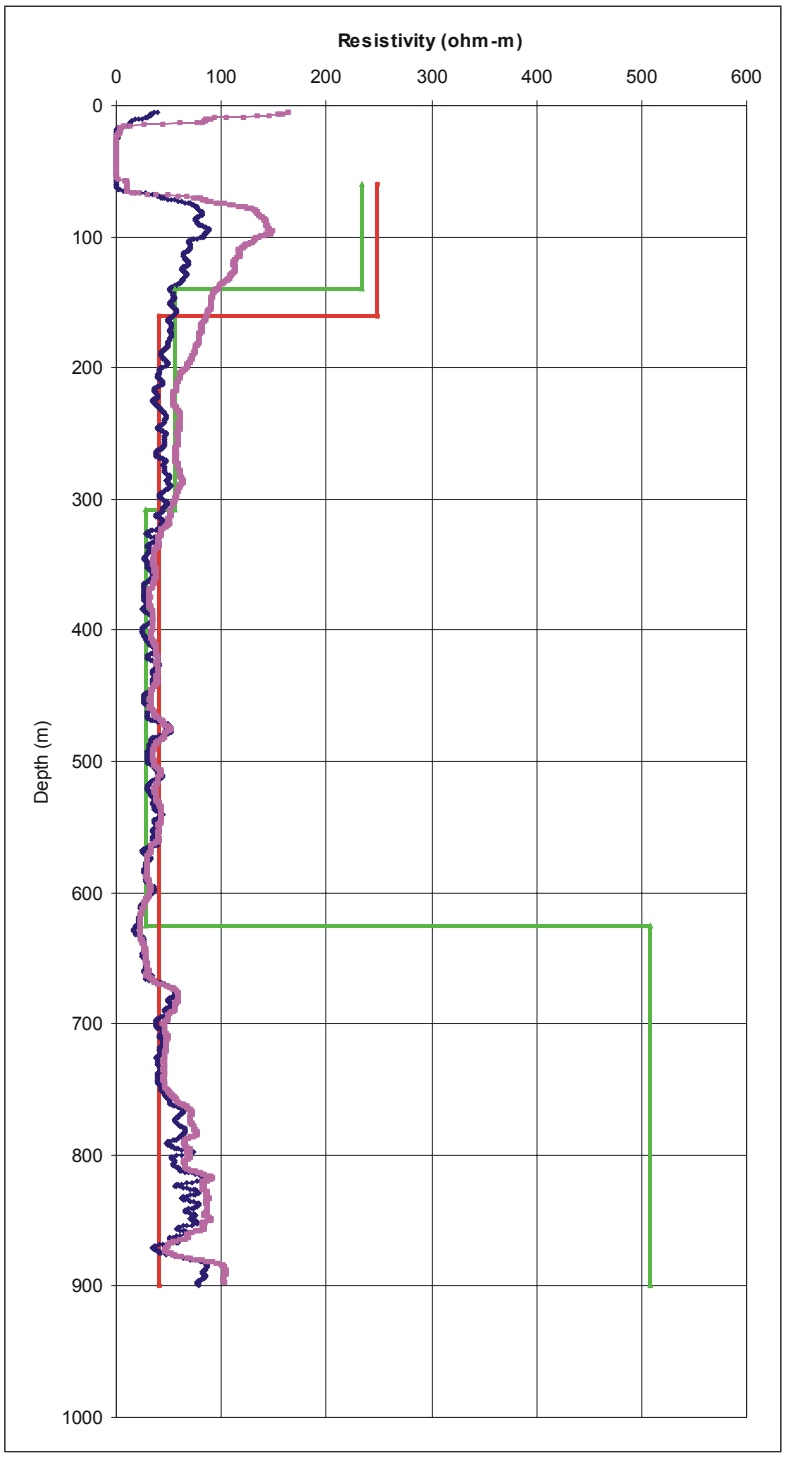

Figure 3-11. Comparison of Electrical Resistivities Modeled at TEM-9 and TEM-10 with Logs for Nye County Early Warning Drilling Program Well 10S: R64 Resistivity Log (Purple), R16 Resistivity Log (Navy Blue), TEM-9 Electrical Resistivity Model (Red), and TEM-10 Electrical Resistivity Model (Green)
NOTE: Scale information provided in meters; for conversion use 1 m = 3.281 ft.

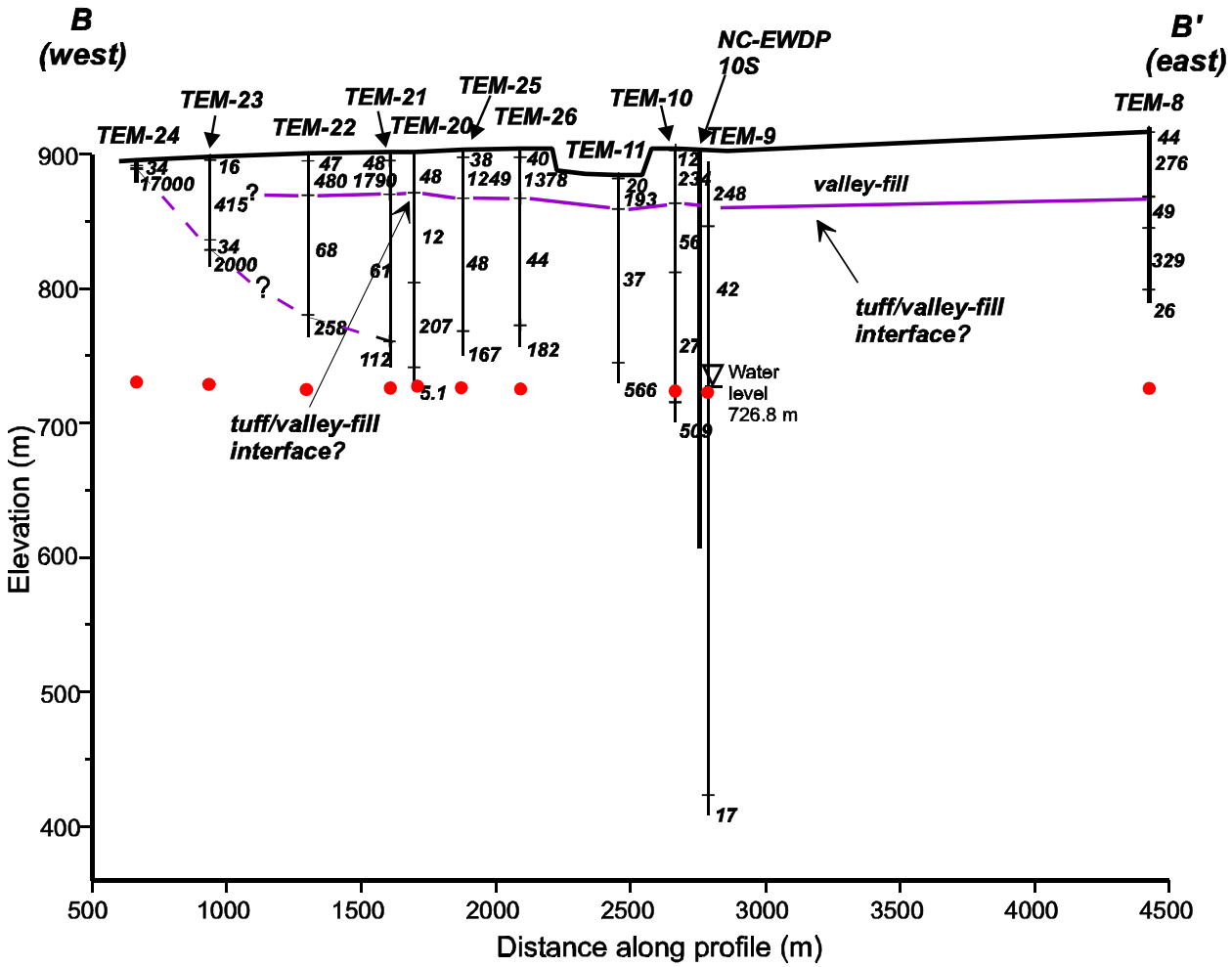

Figure 3-12. Comparison of Estimated Water Table Elevations for Transect B-B' with Estimated Water Table Elevations from Hill, et al. (2002) Represented by Red Dots. Numbers Represent Electrical Resistivities in ohm-m. NC–EWDP Represents Nye County Early Warning Drilling Program.
NOTE: Scale information provided in meters; for conversion use 1 m = 3.281 ft.

The electrical resistivity cross section that results from simultaneous inversion of TEM-12 and IP-3 and single inversion of TEM-15 is shown in Figure 3-13. Also included on the figure for correlation purposes is Well J–12. The model for TEM-12 and IP-3 consists of several distinct layers reflecting lithological variations. In particular, two layers have noticeably high chargeabilities: layers 2 and 4 (see also normalized chargeabilities in Table 3-3). These layers appear to indicate the presence of clay-rich units. Given the uncertainties in modeling parameters, however, the actual normalized chargeabilities indicated for these units may vary from those given in Table 3-3. Note the chargeabilities for the lower units were fixed during the inversion process to a value of 2.0 mV/V. The proximity of TEM-12 and IP-3 to the out cropping tuff units to the west may support mapping the tuff/valley-fill contact. It is currently

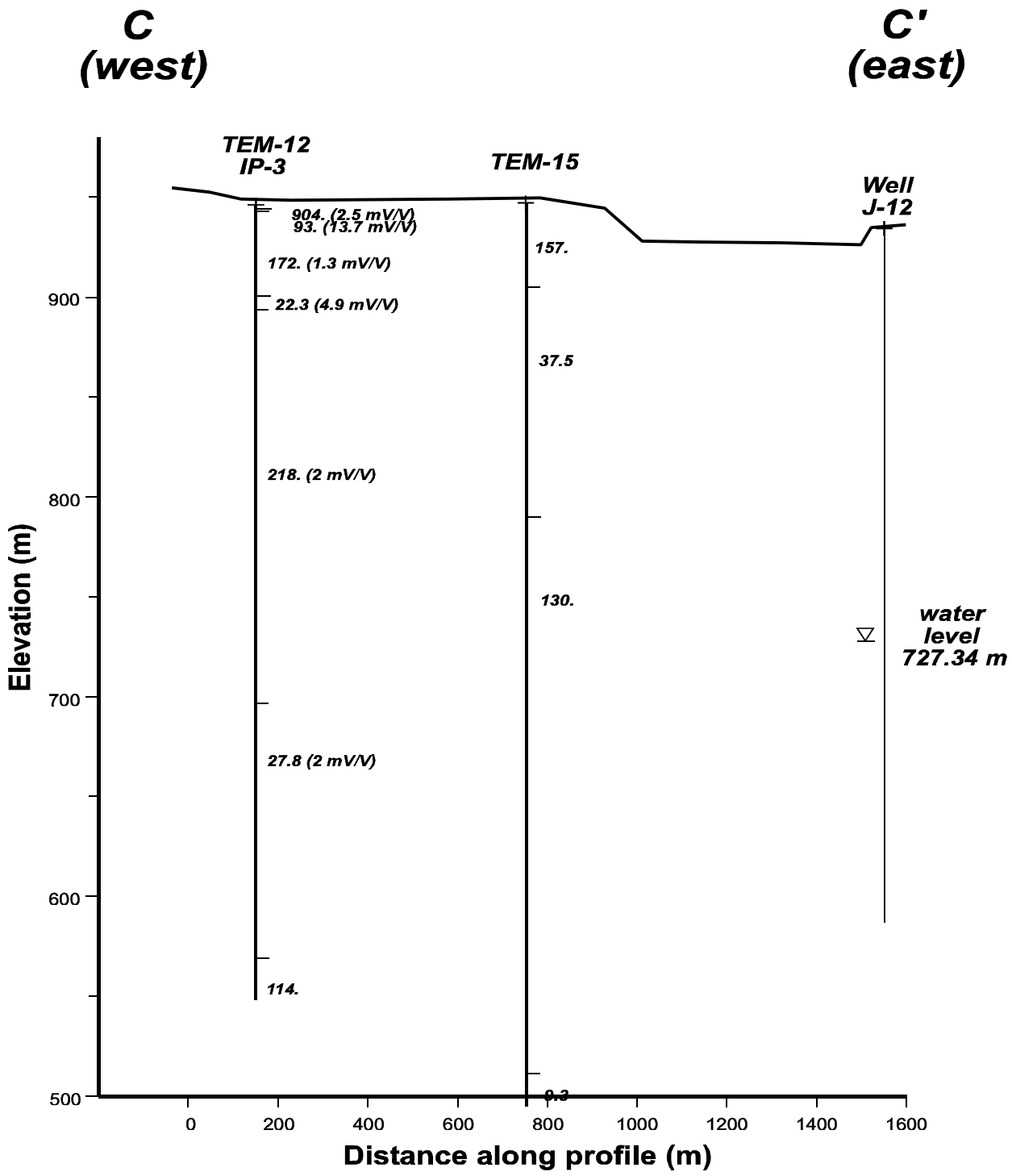

Figure 3-13. Electrical Cross Section for Transect C-C' (see Figure 3-2). Bracketed Numbers Represent Chargeabilities in mV/V, and Numbers without Parentheses Represent Electrical Resistivities in ohm-m.
NOTE: Scale information provided in meters; for conversion use 1 m = 3.281 ft.

Table 3-3. Electrical Resistivity Model for Sounding Station TEM-12/IP-3 Based on Simultaneous Inversion of Time-Domain Electromagnetic Resistivity Sounding Data, Induced Polarization Data, and Schlumberger D.C. Electric Resistivity Depth-Sounding Data

Layer	Electrical Resistivity (ohm-m)	Chargeability (mV/V)	Thickness (m)	Normalized Chargeability (μS/m)×100
1	904	2.5	2.0 [6.6 ft]	0.3
2	93	13.7	0.8 [2.6 ft]	14.7
3	172	1.3	42.7 [140.6 ft]	0.8
4	22.3	4.9	6.7 [22.1 ft]	22.0
5	218	2*	197.0 [646.2 ft]	0.9
6	27.8	2*	—	7.2

*Chargeability values were fixed during the inversion procedure.

not possible to identify which modeled transition represents this interface. Additional information from magnetic surveys performed in the region may support identifying this interface on the model.

Comparison of cross section C-C' with Well J–12 (Figure 3-14) shows the recorded water level does not correlate well with transitions at either station. The transition from high (218 ohm-m) to low (27.8 ohm-m) represents the better station correlation, but the transition is 30–40 m (98–131 ft) lower than the water table elevation at Well J–12 and the water table elevation estimated from the water table elevation contour map of Hill, et al. (2002). The model constructed for TEM15 does not indicate a transition from high to low resistivity that correlates with the measured water table at Well J–12 and that determined from Hill, et al. (2002) (Figure 3-14).

3.3.2.4 Transect D-D'

Transect D-D' trends northeast-southwest and intersects transects B-B' and C-C' (Figure 3-2). This transect is composed solely of time-domain electromagnetic resistivity soundings. These include four 300 × 300-m [984 × 984 ft] transmitter loop soundings (TEM-20, TEM-18, TEM-16, and TEM-15) and two 40 × 40-m [131 × 131-ft] transmitter loop soundings (TEM-17 and TEM-19). Apart from TEM-20, inversion of the remaining soundings generally resulted in poorly resolved models as determined by the orders of magnitude 95-percent confidence intervals Farrell, 2000; Sandberg, 2000) for the model parameters. The cause of the poor resolution of models along this transect is unclear, but may be due to the presence of lateral discontinuities and anthropogenic conductors (e.g., buried cables) in the subsurface.

The electrical resistivity cross section generated by combining the five individual one-dimensional models is shown in Figure 3-15. Also superimposed on the cross section are geological and hydrological data from Wells J–12 and JF–3. The figure shows a possible correlation between the high (greater than 100 ohm-m) to low (less than 25 ohm-m) electrical resistivity transition modeled at stations TEM-18 and TEM-20 and the recorded water levels at Wells JF–3 and J–12. Similar correlations are not observed at stations TEM-15 and

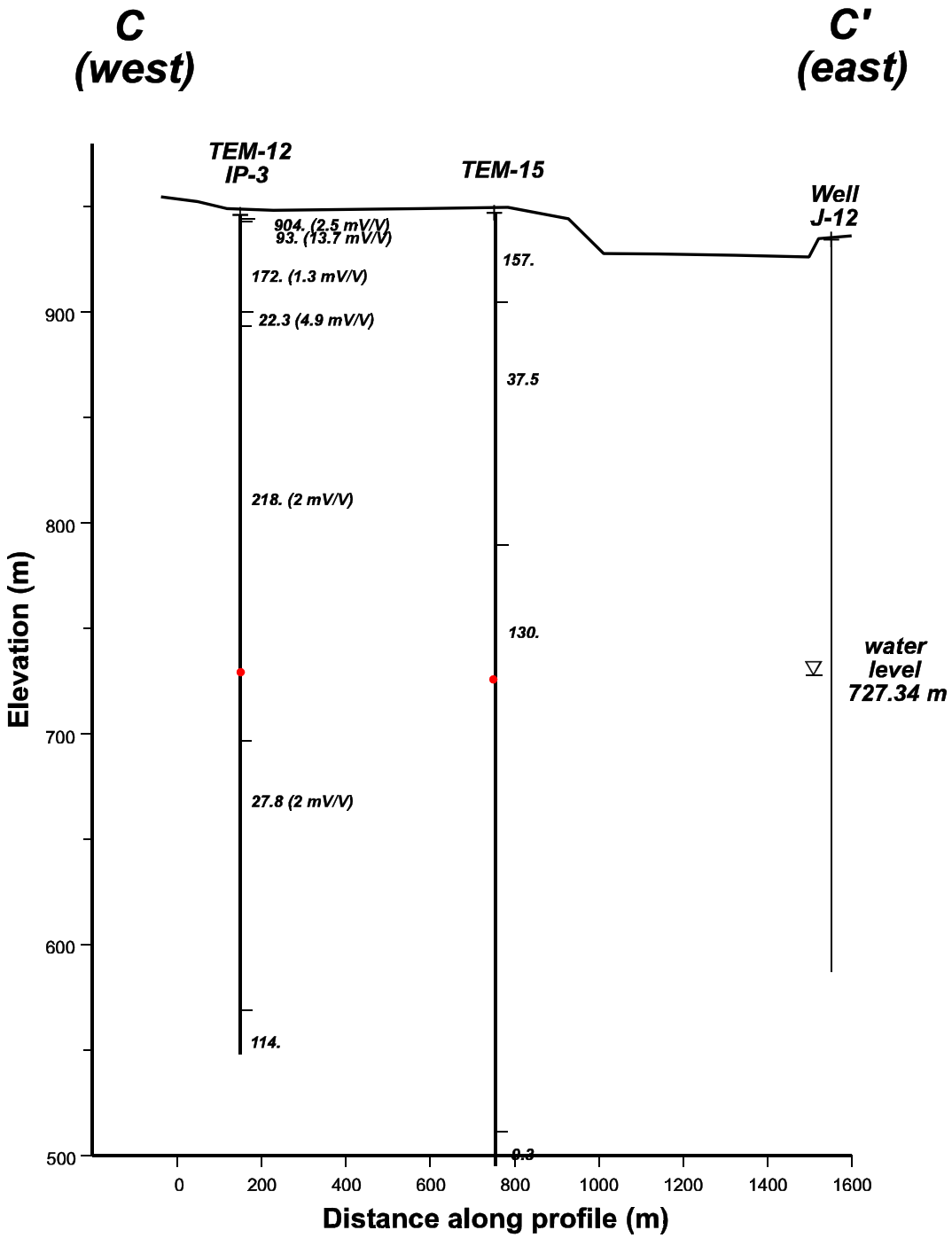

Figure 3-14. Water Table Elevations from Hill, et al. (2002) Represented by Red Dots Superimposed on Electrical Cross Section. Numbers with Parentheses Represent Chargeabilities in mV/V, and Numbers without Parentheses Represent Electrical Resistivities in ohm-m.
NOTE: Scale information provided in meters; for conversion use 1 m = 3.281 ft.

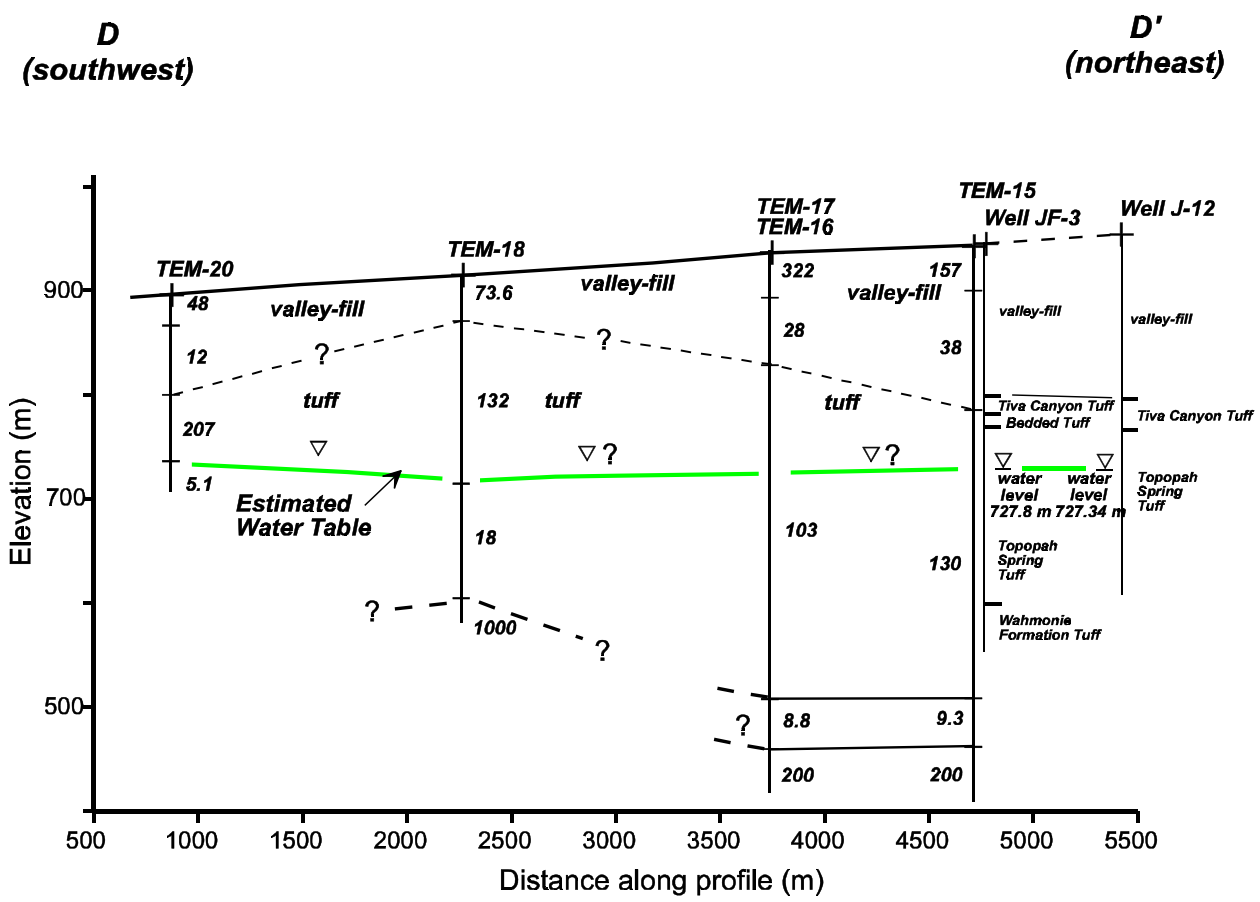

Figure 3-15. Electrical Cross Section for Transect D-D' (see Figure 3-2). Numbers without Parentheses Represent Electrical Resistivities in ohm-m. NOTE: Scale information provided in meters; for conversion use 1 m = 3.281 ft.

TEM-16/17, which are closer to Wells J–12 and JF–3 than TEM-18 and TEM-20. At these stations (TEM-15 and TEM-16/17), a low electrical resistivity layer is modeled at significantly greater depth. Although this may indicate a possible discontinuity in the geological structure, other possible explanations include either model nonuniqueness or the presence of anthropogenic electrically conductive features such as electrical wire in the subsurface. The impacts of nonuniqueness and anthropogenic factors on the models at stations TEM-15 and TEM-16/17 were reflected in the large confidence intervals estimated for model parameters.

Evident on electrical resistivity cross section D-D' is a relatively high electrical resistivity unit *(*$\rho \geq 100$ ohm-m*)* that appears to correlate to the depth of the Tiva Canyon Tuff unit reported in Wells J–12 and JF–3. The cross section indicates the unit appears to attain a maximum elevation in the vicinity of TEM-18. Support for this possible geometry is provided by the aeromagnetic data (Figure 3-2) that indicate a local magnetic high in close proximity to TEM-18. The aeromagnetic data, however, do not support a significant structural discontinuity between TEM-18 and TEM-16/17 (see Figure 3-15) as suggested by the transect. Discussions of available magnetic data for this region are reserved for a followup report on gravity and

magnetic studies in the region. Possible structural discontinuities along this transect also will be addressed further in the followup report that discusses magnetic data collected in the region. The apparent decrease in electrical resistivities modeled along the lateral flanks of the Tiva Canyon Tuff (see TEM-20 model) may reflect either increased saturations because of lateral drainage along the tuff/valley-fill contact or increased clay content above the contact. Unfortunately, no data exist to investigate these possibilities.

The estimated elevation of the water table along D-D' also was compared with the water table contour map of Hill, et al. (2002). The comparison (Figure 3-16) shows the estimated elevations of the water table at TEM-18 and TEM-20 correlate well with the water table contour model of Hill, et al. (2002).

3.3.2.5 Transect E-E'

Transect E-E' extends in a southeasterly direction from the Lathrop Wells cinder cone to the Amargosa Town C Well (Figure 3-2). Recorded water levels at Nye County Early Drilling Program Well 15P and the Amargosa Town C Well are used to evaluate the appropriateness of the models. Transect E-E' includes soundings TEM-1/IP-1, TEM-27/TEM-28, TEM-29/TEM-30/IP-4, TEM-31/TEM-32, and TEM-33/TEM-34, as well as U.S. Geological Survey electrical resistivity soundings USGS 20 and USGS 110 (Greenhaus and Zablocki, 1982). TEM-1/IP-1 and TEM-29/TEM-30/IP-4 allow for simultaneous inversion of time-domain electromagnetic and induced polarization data, while the time-domain electromagnetic pairs permit simultaneous inversion of 300 × 300-m [984 × 984-ft] and 40 × 40-m [131 × 131-ft] time-domain electromagnetic data sets.

Data from USGS 20 and USGS 110 (Greenhaus and Zablocki, 1982) were inverted in this work using a single data set inversion strategy. The electrical resistivity cross section generated for transect E-E' is illustrated in Figure 3-17.

The confidence limits (Farrell, 2000; Sandberg, 2000) on model parameters determined using simultaneous inversion are generally narrow and, therefore, the parameters are viewed as well constrained. As noted earlier, TEM-1/IP-1 is possibly influenced by strong lateral variations in subsurface electrical resistivity and may not provide the true model of the subsurface at the location of the sounding. The upper electrical resistivity layers of model USGS 110 are interpreted as reasonably well constrained based on the narrow 95-percent confidence intervals (Farrell, 2000; Sandberg, 2000). The model developed for USGS 20, although reasonably well constrained, does not detect the water table. The models in transect E-E' generally show upper zone that is electrically resistive, with some localized zones of low electrical resistivity. This high electrical resistivity results from the low moisture content of the valley-fill and lithologic variations. The transition from high to low electrical resistivity modeled at each sounding appears to be relatively consistent and correlates reasonably well with measured water levels at the ends of the transect. Note the difference between the estimated elevation of the water table at TEM-33/TEM-34 and the measured water table elevation at Amargosa Town C Well may reflect the drawdown cone at the Amargosa Town C well. It should be noted also the possibility of clay layers at depth is indicated by the IP-4 Well data (see normalized chargeability of 1.4 mV/V in Table 3-4). Unfortunately, there are no nearby boreholes to support this assertion.

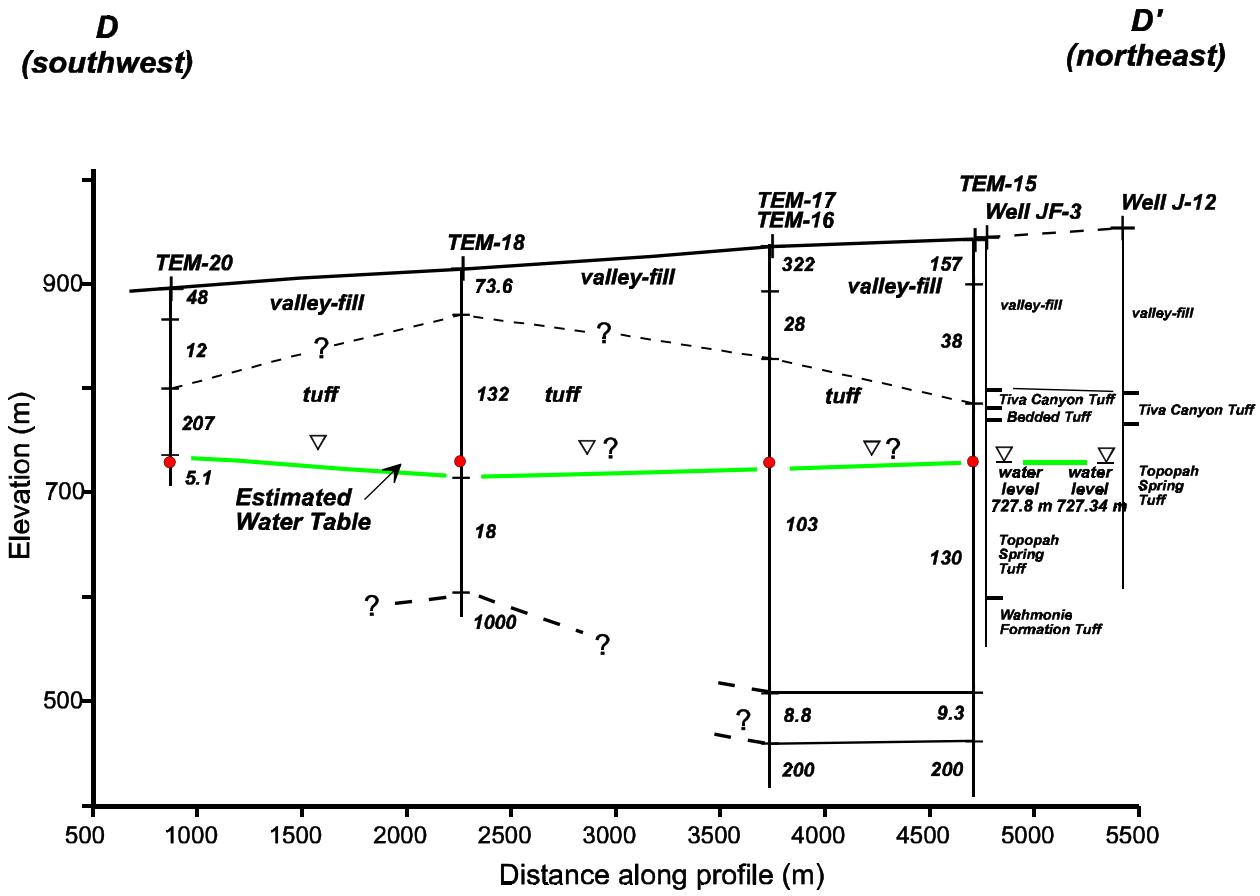

Figure 3-16. Comparison of Estimated Water Table Elevations for Transect D-D' with Estimated Water Table Elevations from Hill, et al. (2002) Represented by Red Dots. Numbers Represent Electrical Resistivities in ohm-m.
NOTE: Scale information provided in meters; for conversion use 1 m = 3.281 ft.

The water table elevation contour map of Hill, et al. (2002) does not include the region traversed by the transect E-E'. Hence, no attempt has been made to validate the inferred water table across the central portion of the cross section.

3.4 Summary

This chapter summarizes the findings of electrical and electromagnetic methods used to map the subsurface electrical resistivity structure of southern Fortymile Wash and northern Amargosa Valley. As noted in the introduction to this chapter, this work has two objectives: (i) to explore the capability of the time-domain electromagnetic resistivity depth-sounding method to map hydrogeologic (including the water table) and geologic targets at depths greater than 100 m [328 ft] in the thick valley-fill and bedrock located south of Yucca Mountain (the

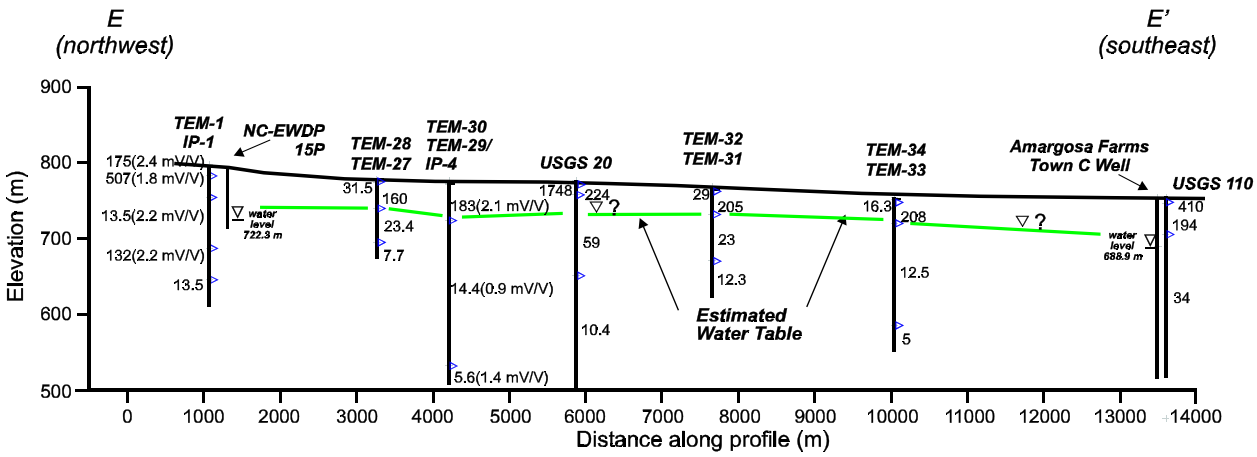

Figure 3-17. Electrical Resistivity Cross Section for Transect E-E' (see Figure 3-2). Numbers with Parentheses Represent Chargeabilities in mV/V, and Numbers without Parentheses Represent Electrical Resistivities in ohm-m. NOTE: Scale information provided in meters; for conversion use 1 m = 3.281 ft.

Table 3-4. Electrical Resistivity Model for Sounding Station TEM-29/TEM-30/IP-3 Based on Simultaneous Inversion of Time-Domain Electromagnetic Resistivity Sounding Data, Induced Polarization Data, and Schlumberger D.C. Electric Resistivity Depth-Sounding Data

Layer	Electrical Resistivity (ohm-m)	Chargeability (mV/V)	Thickness (m)	Normalized Chargeability (μS/m) × 100
1	183	2.1	47.6 [156.3 ft]	1.2
2	14.4	0.9	190.5 [625 ft]	6.4
3	5.6	1.4	—	25.0

1998 survey); and (ii) based on successful completion of the first objective to identify a suite of geophysical tools, including the time-domain electromagnetic resistivity depth-sounding method, to map hydrogeologic and geologic targets important for assessing repository safety in the data-sparse region south and east of the proposed repository location (the 1999 survey).

To address the first objective, a time-domain electromagnetic resistivity depth sounding survey was performed between the Nevada Test Site and the community of Amargosa Farms (Figure 3-2). The results produced an electrical resistivity cross section of the subsurface that showed reasonable correlation with data obtained from several sources. Although the cross section reproduced some known large-scale geologic trends of the region, the predictive accuracy the cross section produced was limited because of limited modeling and data constraints. Uncertainty in the water table elevations inferred from modeling the time-domain electromagnetic data is comparable with the range in water table elevations {~20 m [66 ft]} measured along the portion of the transect north of U.S. Highway 95 (refer to the water table

elevation contour map of Hill, et al., 2002). Nevertheless, decrease in the water table elevation from north to south seen on the map is reproduced on the cross section.

Based on the potential of the time-domain electromagnetic resistivity depth-sounding approach to map hydrologic targets south of Yucca Mountain, the method was included in a suite of geophysical techniques that included induced polarization and Schlumberger D.C. electrical resistivity depth sounding to map hydrologic and geologic targets in southern Fortymile Wash and northern Amargosa Valley. By using data from these varied sources, additional constraints were included in the modeling process to improve subsurface characterization.

This suite of measurements was included in a series of electrical resistivity surveys performed in southern Fortymile Wash and northern Amargosa Valley (Figure 3-2) during 1999. Based on the collected data, results from the five transects generated showed the hydrogeologic and geologic information provided by the survey demonstrated reasonable correlation with independent sources of data. Where this suite of survey techniques was not used and where additional modeling constraints were not available, poor model resolution and modeling nonuniqueness effects, illustrated by large parameter uncertainties, were generally observed. In several instances, models generated for these conditions correlated poorly with independent sources of data (i.e., borehole data and groundwater elevations). Although the modeling results obtained from the 1999 survey were generally more accurate compared with the 1998 survey, the accuracy of water table estimates made using 1999 survey results were still found to be less than that required to improve current interpretations of water table elevations at Yucca Mountain. Trends in the water table elevations inferred from the modeling, however, were qualitatively consistent with field measurements and current water table contour maps. It is possible that some differences between water table elevations estimated from the geophysical approach and those measured at monitoring wells may be because of phenomena such as capillary fringe rise above the water table. Such rises, which are largest in fine-grained soils, may extend several meters above the water table. Although the capillary fringe is not considered part of the saturated zone, the fringe zone is, nevertheless, fully saturated and, as a result, is expected to display electrical properties identical to the region below the water table. Hence, capillary fringe effects and near-saturated conditions above the water table may result in an estimated water table elevation above the measured water table elevation.

Although of limited usefulness to support water table mapping, the integrated modeling strategy also supported delineation of hydrostratigraphic units. In particular, the presence of clay units interpreted in the transects appears to be confirmed by induced polarization measurements. These units, which represent low permeability zones, can be incorporated into the hydrostratigraphic framework model for the region and subsequently included in the groundwater flow and transport simulations for the region. This approach can be interpreted as supporting the evaluation of alternate models of flow and transport through the region. Other hydrostratigraphic delineations also appear to be illustrated in the transect profiles. These potential interfaces will be further explored in a followup report on gravity and magnetic studies in the region. Results from these two reports are expected to yield an improved hydrostratigraphic characterization of the region. This improved characterization could lead to greater constraints on groundwater flow paths through southern Fortymile Wash and northern Amargosa Valley.

4 CONCLUSIONS AND FUTURE WORK

Two general conclusions can be drawn from this work.

- Results from the electrical resistivity mapping studies described in this report show the simultaneous inversion of multiple geophysical data sets approach has the potential to produce an electrical resistivity map of the subsurface that correlates well with hydrologic and geologic data obtained from independent sources. Although the maps developed in this study reproduced the large-scale geologic and hydrologic trends of the region, the accuracy the cross-sectional models produced is viewed as insufficient to support water table mapping at the level of accuracy required to improve existing water table interpretations.

- Although the integrated suite of electrical measurements performed in this study may not support quantitatively accurate water table mapping, the integrated approach appears to have the potential to support hydrostratigraphic mapping of geologic units that are electrically distinct at a level of accuracy that may support inclusion in hydrogeologic models. This supposition has not been verified. This mapping capability, if combined with other geophysical mapping techniques and available geologic data, can lead to an improved understanding of the geologic and hydrogeologic structures of southern Fortymile Wash and northern Amargosa Valley.

4.1 Future Work

On the basis of studies summarized in this report two possible areas of future analyses can be identified to make use of the existing data and interpretations. These are summarized next.

- Use existing gravity and magnetic data for southern Fortymile Wash and northern Amargosa Valley, along with geological data from the Nye County Early Warning Drilling Program, to develop (or improve) models for the region southeast of Yucca Mountain. These models can be used to support hydrologic modeling across southern Fortymile Wash and northern Amargosa Valley and delineation of the tuff/valley-fill contact required for performance assessment calculations.

- Update the NRC and CNWRA hydrostratigraphic framework model (Sims, et al., 1999) using the models based on recent electrical resistivity, magnetic, and gravity surveys.

5 REFERENCES

Blakely, R.J., V.E. Langerheim, D.A. Ponce, and G. Dixon. "Aeromagnetic Survey of the Amargosa Desert, Nevada, and California: A Total for Understanding Near-Surface Geology and Hydrology." U.S. Geological Survey Open-File Report 00-188. 2000.

Brocher, T.M., F.E. Hart, and S.F. Carle. "Feasibility Study of the Seismic Reflection Method in Amargosa Desert, Nye County, Nevada." U.S. Geological Survey Open-File Report 89-133. 1990.

Carr, W.J., J.A. Grow, and S.M. Keller. "Lithologic and Geophysical Logs of Drill Holes Felderhoff Federal 5-1 and 25-1, Amargosa Desert, Nye County, Nevada." U.S. Geological Survey Open-File Report 95-155. 1995.

CRWMS M&O. "Saturated Zone Flow and Transport Process Model Report." TDR–NBS–HS–000001. Rev. 00. Las Vegas, Nevada: CRWMS M&O. 2000.

Farrell, D.A. "Scientific Notebook #317E: Subsurface Electrical Conductivity Mapping of Fortymile Wash and the Amargosa Desert (03/18/1999–02/28/2000)." San Antonio, Texas: CNWRA. 2000.

Farrell, D.A., P. LaFemina, A. Armstrong, S. Sandberg, and N. Rogers. "Constraining Hydrogeologic Models Using Geophysical Techniques: Case Study—Fortymile Wash and Amargosa Desert, Southern Nevada." Proceedings of the Symposium on the Application of Geophysics to Engineering and Environmental Problems, Arlington, Virginia. M. Powers, A. Ibrahim, and L. Cramer, eds. Denver, Colorado: Environmental and Engineering Geophysical Society. pp. 213–222. 2000.

Farrell, D.A., A. Armstrong, J.R. Winterle, D.R. Turner, D.A. Ferrill, J.A. Stamatakos, N. Coleman, M.B. Gray, and S.K. Sandberg. "Structural Controls on Groundwater Flow in the Yucca Mountain Region." San Antonio, Texas: CNWRA. 1999.

Greenhaus, M.R. and C.J. Zablocki. "A Schlumberger Resistivity Survey of the Amargosa Desert, Southern Nevada." U.S. Geological Survey Open-File Report 82-897. 1982.

Hill, M., J.R. Winterle, and R. Green. "Revised Site-Scale Potentiometric Surface Map for Yucca Mountain, Nevada." San Antonio, Texas: CNWRA. 2002.

Hoover, D.B,, M.P. Chornack, and M.M. Broker. "E-Field Ratio Telluric Traverses Near Fortymile Wash, Nevada Test Site, Nevada." U.S. Geological Survey Open-File Report 82-1042. 1982.

Lipman, P.W. and E.J. Mackay. "Geologic Map of the Topopah Spring SW Quadrangle, Nye County, Nevada." U.S. Geological Survey Geological Quadrangle Map, GQ–439. Scale 1:24,000. 1965.

Meju, M.A. "A Simple Method of Transient Electromagnetic Data Analysis." *Geophysics*. Vol. 63, No. 2. pp. 405–410. 1998.

Mohanty, S., T.J. McCartin, and D.W. Esh. "Total-system Performance Assessment (TPA) Version 4.0 Code: Module Descriptions and User's Guide." San Antonio, Texas: CNWRA. 2000.

Oatfield, W.J. and J.B. Czarnecki. "Hydrogeologic Inferences from Drillers' Logs and from Gravity and Resistivity Surveys in the Amargosa Desert, Southern Nevada." U.S. Geological Survey Open-File Report 89-234. 1989.

Reamer, C.W. "U.S. Nuclear Regulatory Commission/U.S. Department of Energy Technical Exchange and Management Meeting on Unsatured and Saturated Flow Under Isothermal Conditions (October 31–November 2, 2000)." Letter (November 17) to S.J. Brocoum, DOE. Washington, DC: NRC. 2000a. <http://www.nrc.gov/waste/hlw-disposal/public-involvement/mtg-archive.html#KTI>

Reamer, C.W. "U.S. Nuclear Regulatory Commission/U.S. Department of Energy Technical Exchange and Management Meeting on Radionuclide Transport (December 5–7, 2000)." Letter (November 17) to S.J. Brocoum, DOE. Washington, DC: NRC. 2000b. <http://www.nrc.gov/waste/hlw-disposal/public-involvement/mtg-archive.html#KTI>

Sandberg, S.K. "Final Report: Geophysical Survey at Fortymile Wash, Yucca Mountain, Nevada: Geophysical Solutions." San Antonio, Texas: CNWRA. 2000.

———. "Draft Report on Modeling TEM Data from Nevada: Geophysical Solutions." Albuquerque, New Mexico: Geophysical Solutions. 1998a.

———. "Inverse Modeling Software for Resistivity, Induced Polarization (IP), and Transient Electromagnetic (TEM, TDEM) Soundings: Manual for Computer Programs, ZONGE, READZONG, T47INPUT, READ, SLUMBER, RAMPRES3, EINVRT6 (MS-DOS Version 6.0)." Albuquerque, New Mexico: Geophysical Solutions. 1998b.

———. "Examples of Resolution Improvement in Geoelectrical Soundings Applied to Groundwater Investigations." *Geophysical Prospecting.* Vol. 41. pp. 207–227. 1993

Sharma, P.V. *Environmental and Engineering Geophysics*. Cambridge, United Kingdom: Cambridge University Press. 1997.

Sims, D.W., J.A. Stamatakos, D.A. Ferrill, H.L. McKague, D.A. Farrell, and A. Armstrong. "Three-Dimensional Structural Model of the Amargosa Desert, Version 1.0: Report to Accompany Model Transfer to the Nuclear Regulatory Commission. San Antonio, Texas: CNWRA. 1999.

Slater, L.D. and D. Lesmes. "IP Interpretation in Environmental Investigations." *Geophysics*. Vol. 67, No. 1. pp. 77–88. 2002.

Winterle, J.R. "Evaluation of Alternative Concepts for Saturated Zone Flow: Effects of Recharge and Water Table Rise on Flow Paths and Travel Times at Yucca Mountain." San Antonio, Texas: CNWRA. 2003.

Winterle, J.R., M.E. Hill, and C. Manepally. "Concepts of Saturated Zone Modeling for Development of a Site-Scale Groundwater Flow Model for Yucca Mountain." San Antonio, Texas: CNWRA. 2002.

APPENDIX

ELECTRICAL RESISTIVITY MODELS USED TO SUPPORT FIGURES

This appendix contains the data used to construct the models presented in this report. Note station locations presented are based on both differential Global Positioning System measurements and map information. Differential Global Positioning System was used to establish the UTM–X and UMT–Y locations of the measurement stations, and station elevations were inferred from existing U.S. Geological Survey 15- and 7.5-minute series maps of the region. Maps used from this series include Amargosa Valley, Nevada, 1983; Big Dune, Nevada, 1986; Busted Butte, Nevada 1983; and Lathrop Wells, Nevada, 1961.

Table 1a. Transect F-F' Time-Domain Electromagnetic Station Locations

Station	UTM–X (m)*	UTM–Y (m)*	Elevation (m)*
A	550,680	4,045,799	734.9
B	553,039	4,052,576	786.4
C	553,070	4,053,930	797.1
E	553,280	4,056,330	819.0
F	553,301	4,057,646	831.2
G	553,429	4,058,250	837.3
H	553,370	4,059,330	846.7
I	553,670	4,060,130	854.7
J	554,220	4,061,530	865.6
K	553,845	4,063,732	892.8

*Note: [1 m = 3.28 ft]

Table 1b. Transect F-F' TEM* Models Based on Data Inversion

Depth (m)†	Electrical Resistivity (ohm-m)	Depth (m)	Electrical Resistivity (ohm-m)
Station A		**Station B**	
0–29	1,770	0–28	1,719
29–48	24	28–57	47
>48	9.8	57–168	22
—	—	>168	5.8
Station C		**Station E**	
0–27	1,752	0–34	798
27–55	45	34–85	62
55–141	24	85–129	25
>141	6	>129	4.7
Station F		**Station G**	
0–34	1,046	0–34	1,845
34–90	67	34–117	68
90–112	21	117–122	2.6
>112	7.3	>122	25

Table 1b. Transect F-F' TEM* Models Based on Data Inversion (continued)			
Depth (m)†	**Electrical Resistivity (ohm-m)**	**Depth (m)**	**Electrical Resistivity (ohm-m)**
Station H		**Station I**	
0–31	1,621	0–35	1,313
31–124	71	35–141	66
124–126	3.3	>141	13.3
>126	16.5	—	—
Station J		**Station K**	
0–40	982	0–39	1,067
40–141	63	39–132	68
>141	15	>132	22

*TEM — time-domain electromagnetic
†Note: [1 m = 3.28 ft]

Table 2a. Stations Along Cross Section A-A’			
Station	**X (m)***	**Y (m)***	**Elevation (m)***
4	543,130	4,060,860	841.2
1	544,736	4,059,006	792.5
2	546,700	4,058,850	805.3
USGS 18†	—	—	—
IP-2	548,050	4,057,600	805.6
3	548,050	4,057,600	805.6
3A	548,050	4,057,600	805.6
5	550,075	4,057,275	813.8
6	551,189	4,057,024	816.8
USGS 19†	—	—	—
7	552,650	4,056,750	821.2

*Note: [1 m = 3.28 ft]
†Greenhaus, M.R. and C.J. Zablocki. “A Schlumberger Resistivity Survey of the Amargosa Desert, Southern Nevada.” U.S. Geological Survey Open-File Report 82-897. 1982.

Table 2b. Transect A-A’		
Depth (m)*	**Electrical Resistivity (ohm-m)**	**IP (mV/V)†**
Station TEM-1‡ and IP-1		
0–0.96	1,440.60	0.49
0.96–2.22	1,235.77	2.67
2.22–15.19	174.81	2.44
15.19–42.52	507.57	1.80
42.52–110.54	13.50	2.2§
110.54–151.4	131.84	2.2§
>151.4	13.46	2.2§
Station TEM-4		
0–3.38	50.71	—
3.38–105.6	1,191.42	—
105.6–200.45	21.29	—
>200.45	5.53	—
Station TEM-5		
0-82.74	92.18	—
82.74–367.44	24.59	—
367.44–393.86	29.27	—
>393.86	5.43	—
Station TEM-7		
0–114.02	80.99	—
114.02–265.85	7.54	—
>265.85	19.67	—

Table 2b. Transect A-A' (continued)		
Depth (m)*	**Electrical Resistivity (ohm-m)**	**IP (mV/V)†**
Station USGS 18		
0–2.54	885.10	
2.54–32.29	246.45	
32.29–188.43	53.31	
188.43–668.6	15.59	
Station TEM-2		
0–75.60	100.36	—
75.60–180.68	11.14	—
180.68–287.45	666.08	—
Station TEM-3/TEM-3A		
0–1.15	36.45	—
1.15–78.27	104.70	—
78.27–106.54	18.63	—
106.54–182.07	86.12	—
>182.07	8.26	—
>287.45	9.29	—
Station IP-2		
0–1.73	832.67	3.0
1.73–4.82	106.52	4.91
4.82–70.9	188.20	1.52
>70.9	52.97	7.86
Station TEM-6		
0–109.16	87.94	—
109.16–259.11	13.19	—
>259.11	18.0	—
Station USGS 19		
0–334	435.91	—
3.34-15.16	213.98	—
15.16–28.32	432.47	—
20.32–118.28	91.32	—
118.28–1,081.03	23.31	—
>1,081.03	30.64	—

*Note: [1 m = 3.28 ft]
†IP — induced polarization (unit mV/V = millivolt per volt)
‡TEM — time-domain electromagnetic
§ Chargeability values fixed during inversion process

Table 3a. Stations Along Cross Section B-B’			
Station	**X (m)***	**Y (m)***	**Elevation (m)***
24	551,080	4,065,000	894.9
23	551,380	4,065,000	896.1
22	551,680	4,065,000	898.6
21	551,980	4,065,000	900.7
20	552,130	4,064,850	899.5
25	552,346	4,064,956	901.9
26	552,504	4,064,927	902.2
11	552,868	4,065,324	895.2
10	553,068	4,065,112	904.6
9	553,218	4,064,962	904.6
8	554820	4,056,750	913.5
*Note: [1 m = 3.28 ft]			

Table 3b. Transect B-B’		
Depth (m)*	**Electrical Resistivity (ohm-m)**	**IP (mV/V)†**
Station 24		
0–2.77	26.31	—
2.77–11.52	273.69	—
>11.52	15,552.67	—
Station 23		
0–2.14	16.27	—
2.14–61.34	415.27	—
61.34–68.87	34.29	—
>68.87	2,000.0	—
Station 22		
0–5.55	46.59	—
5.55–31.19	479.64	—
31.19–114.16	67.86	—
>114.16	258.30	—
Station 21		
0–6.63	48.01	—
6.63–31.49	1,90.47	—
31.49–140.84	60.73	—
>140.84	112.46	—

Table 3b. Transect B-B' (continued)		
Depth (m)*	**Electrical Resistivity (ohm-m)**	**IP (mV/V)†**
Station 20		
0–30.49	47.72	—
30.49–97.15	12.18	—
97.15–160.16	206.98	—
>160.16	5.13	—
Station 25		
0–5.37	37.93	—
5.37–36.06	1,249.07	—
36.06–134.82	48.20	—
>134.82	167.18	—
Station 26		
0–6.42	39.83	—
6.42–37.0	1,378.16	—
37.0–131.33	43.95	—
>131.33	181.60	—
Station 11		
0–2.41	19.80	—
2.41–25.0	193.33	—
25.0–189.28	37.15	—
>189.28	565.64	—
Station 9		
0–48.92	248.08	—
48.92–471.78	41.64	—
>471.78	17.21	—
Station 8		
0–3.97	43.54	—
3.97–51.92	275.64	—
51.92–75.22	48.56	—
75.22–121.14	328.55	—
>121.14	25.71	—

*Note: [1 m = 3.28 ft]
†IP — induced polarization (unit mV/V = millivolt per volt)

Table 4a. Stations Along Cross Section C-C’			
Station	**X (m)***	**Y (m)***	**Elevation (m)***
12	552,910	4,068,390	944.0
15	553,650	4,068,400	946.4
IP-3	552,769	4,068,528	946.4
*Note: [1 m = 3.28 ft]			

Table 4b. Transect C-C’		
Depth (m)*	**Electrical Resistivity (ohm-m)**	**IP (mV/V)†**
Station TEM-12‡ and IP-3		
0–2.01	903.77	2.53
2.01–2.79	92.87	13.74
2.79–45.53	171.80	1.26
45.53–52.26	22.31	4.91
52.26–249.23	218.10	2.0§
249.23–376.85	27.75	2.0§
>376.85	114.28	2.0§
Station TEM-15		
0–41.98	157.38	—
41.98–157.29	37.50	—
157.29–435.65	130.18	—
435.65–482.06	9.31	—
>482.06	200.0	—

*Note: [1 m = 3.28 ft]
†IP — induced polarization (unit mV/V = millivolt per volt)
‡TEM — time-domain electromagnetic
§ Chargeability values fixed during the inversion process

Table 5a. Stations Along Cross Section D-D’			
Station	**X (m)***	**Y (m)***	**Elevation (m)***
20	552,130	4,064,850	899.5
18	532,690	4,066,170	916.8
16	553,500	4,067,360	934.2
17	553,390	4,067,470	935.4
15	553,650	4,068,400	946.4
*Note: [1 m = 3.28 ft]			

Table 5b. Transect D-D’		
Depth (m)*	**Electrical Resistivity (ohm-m)**	**IP (mV/V)†**
Station TEM-20‡		
0–30.49	47.72	—
30.49–97.15	12.18	—
97.15–160.16	206.98	—
>160.16	5.13	—
Station TEM-18		
0–43.07	73.5	—
43.07–201.43	132.15	—
201.43–310.78	17.90	—
310.78	1,000.00	—
Station TEM-6 and TEM-17		
0–45.40	321.89	—
45.40–107.99	27.88	—
107.99–429.52	102.87	—
429.52–478.52	8.77	—
478.52	200.00	—
Station TEM-15		
0–41.98	157.38	—
41.98–157.29	37.50	—
157.29–435.65	130.18	—
435.65–482.06	9.31	—
>482.06	200.00	—

*Note: [1 m = 3.28 ft]
†IP — induced polarization (unit mV/V = millivolt per volt)
‡TEM — time-domain electromagnetic

Table 6a. Stations Along Cross Section E-E'			
Station	**X (m)***	**Y (m)***	**Elevation (m)***
1	554,736	4,059,006	792.5
IP-1	554,736	4,059,006	792.5
27	544,753	4,056,625	778.2
28	544,623	4,056,746	778.2
29	545,100	4,055,732	776.0
30	544,977	4,055,862	776.0
IP-4	544,977	4,055,862	776.0
USGS 20†	—	—	—
31	547,220	4,052,850	768.1
32	547,175	4,052,666	768.1
33	547,446	4,050,363	752.8
34	547,316	4,050,233	752.8

*Note: [1 m = 3.28 ft]

†Greenhaus, M.R., and C.J. Zablocki. "A Schlumberger Resistivity Survey of the Amargosa Desert, Southern Nevada." U.S. Geological Survey Open-File Report 82-897. 1982.

Table 6b. Transect E-E'		
Depth (m)*	**Electrical Resistivity (ohm-m)**	**IP (mV/V)†**
Station TEM-1‡ and IP-1		
0–0.96	1,440.60	0.49
0.96–2.22	1,235.77	2.67
2.22–15.19	174.81	2.44
15.19–42.52	507.57	1.80
42.52–110.54	13.50	2.2
110.54–151.4	131.84	2.2
>151.4	13.46	2.2
Station TEM-27 and TEM-28		
0–3.34	31.51	—
3.34–37.61	160.02	—
37.61–82.49	23.40	—
>82.49	7.71	—
Station TEM2-9, TEM-30, and IP-4		
0–0.9	728.19	1.88
0.9–2.03	1,158.67	3.89
2.03–2.23	4.49	2.84
2.23–3.55	2,002.38	0.94
3.55–4.38	8.90	0.72
4.38–52.02	182.61	2.13
52.02–242.52	14.38	0.90
>242.52	5.56	1.36

Table 6b. Transect E-E' (continued)		
Depth (m)*	**Electrical Resistivity (ohm-m)**	**IP (mV/V)†**
USGS 20		
0–2.55	1,748.34	—
2.55–18.08	224.08	—
18.08–124.24	59.08	—
124.24–1,325.5	10.44	—
>1,325.5	210.16	—
Station TEM-31 and TEM-32		
0–4.13	28.95	—
4.13–36.07	204.73	—
36.07–96.92	22.66	—
>96.02	12.27	—
Station TEM-33 and TEM-34		
0-2.26	16.30	—
2.26–34.08	208.00	—
34.08–167.56	12.48	—
>167.56	5.01	—
USGS 110		
0–7.07	410.41	—
7.07–48.31	194.04	—
48.31–289.54	34.09	—
209.54–1,167.86	11.35	—
>1,156.86	109.58	—

*Note: [1 m = 3.28 ft]
†IP — induced polarization (unit mV/V = millivolt per volt)
‡TEM — time-domain electromagnetic

References

U.S. Geological Survey. "Big Dune Quadrangle, Nevada, Nye County." U.S. Geological Survey Geological Topographic 7.5-Minute Series Map. Provisional Edition. Scale 1:24,000. 1986.

———. "Amargosa Valley Quadrangle, Nevada, Nye County." U.S. Geological Survey Geological Topographic 7.5-Minute Series Map. Scale 1:24,000. 1983.

———. "Busted Butte Quadrangle, Nevada, Nye County." U.S. Geological Survey Geological Topographic 7.5-Minute Series Map. Scale 1:24,000. 1983.

———. "Lathrop Wells Quadrangle, Nevada, Nye County." U.S. Geological Survey Geological Topographic 15-Minute Series Map. Scale 1:62,500. 1961.